CHAPTER 1 INTRODUCTION AND LITERATURE REVIEW

1.1. Introduction

Frequency Selective Surfaces (FSSs) are specialized structures featuring periodically arranged metal patches or slots that are etched onto a metal surface and supported by a dielectric material (Fig. 1.1.1). The collective response of the periodic array is intricately linked to the design of the unit-cell and the spatial separation between these cells. The unique capability of FSSs to selectively manipulate electromagnetic (EM) waves based on their frequency renders them invaluable in various applications.

The frequency tunable properties of FSSs make them versatile components in spatial filters, absorbers, dichroic sub-reflectors, and electromagnetic wave polarizers, catering to both commercial and defense applications. Their adaptability in shaping and controlling electromagnetic waves has positioned them as crucial elements in diverse technological contexts [1].

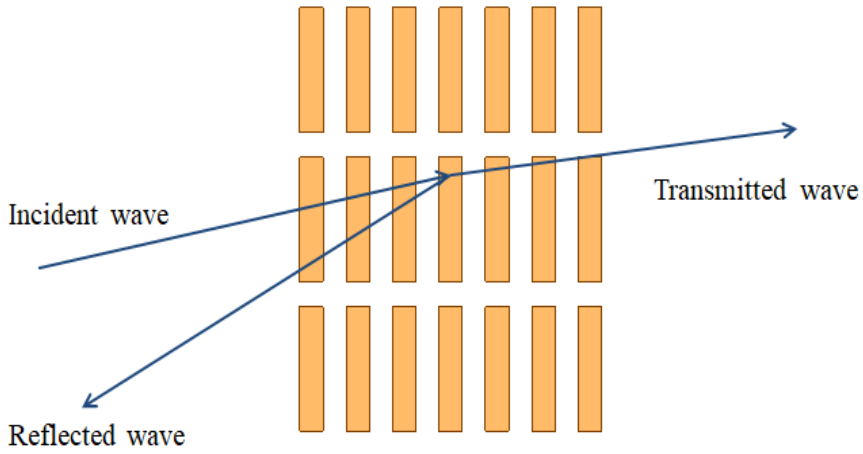

Fig. 1.1.1. Periodic array consists of metal strips.

While FSSs share a theoretical similarity with classical two-port devices, their practical design is notably complex. This complexity arises from the demanding task of achieving specific filter characteristics tailored for different angles of incidence and

wave polarizations. Unlike simpler devices, FSSs require a meticulous design approach to ensure optimal performance across a spectrum of conditions. This intricate design challenge underscores the importance of precision in configuring FSSs for diverse operational scenarios, emphasizing the need for careful consideration and engineering expertise in their implementation.

When an electromagnetic plane wave interacts with a periodic array, certain phenomena occur in terms of reflection and transmission. The incident wave can be divided into two components: one that is transmitted in the forward direction and another that is reflected in the specular direction. The behavior of these waves is particularly interesting under resonant conditions.

Under resonant conditions, the amplitude of the reflected wave (Er) or the amplitude of the transmitted wave (Et) may become equal to the amplitude of the incident wave (Ei). This resonance indicates a specific condition where the waves interact with the periodic array in a way that enhances either the reflection or transmission.

To quantify these interactions, reflection coefficient (Γ) and transmission coefficient (τ) are defined. The reflection coefficient (Γ) represents the ratio of the amplitude of the reflected wave (Er) to the amplitude of the incident wave (Ei), expressed as:

$$\Gamma = \frac{E_r}{E_i} \tag{1.1}$$

Similarly, the transmission coefficient (τ) represents the ratio of the amplitude of the transmitted wave (Et) to the amplitude of the incident wave (Ei), and it is given by:

$$\tau = \frac{E_t}{E_i} \tag{1.2}$$

These coefficients provide a quantitative measure of how much of the incident wave is being reflected and transmitted by the periodic array. Under resonant conditions, if either the reflection coefficient (Γ) or the transmission coefficient (τ) becomes equal to 1, it implies complete reflection or transmission, respectively. Resonance conditions play a crucial role in optimizing the performance of periodic arrays in various applications.

1.2. A Brief History of Periodic Surfaces

The exploration of periodic surfaces, a field that gained momentum in the mid-1960s, was initially motivated by significant potential applications in the military sector. However, the fundamental principles behind periodic surfaces had been understood long before this period. In 1919, a patent was granted to the renowned figures Marconi and Franklin for their pioneering work on parabolic wire section reflectors. They introduced the concept of "tuned elements," proposing that the section length should ideally be half the operating wavelength. They further suggested that this length could be adjusted by incorporating inductors or capacitors, showcasing an early understanding of tuning mechanisms for optimizing performance [1].

In 1974, B. A. Munk was granted a patent that contributed to the evolving knowledge in this area. Munk proposed a crucial idea for a periodic surface to exhibit a stable resonant frequency concerning the angle of incidence. According to Munk, the interelement spacings, or the distances between the components of the periodic surface, must be relatively small to achieve stable resonant frequencies. This insight laid the groundwork for designing and understanding periodic surfaces with specific resonant characteristics, marking a significant step forward in the field [1].

The historical development outlined here highlights the early recognition of the potential of periodic surfaces, with notable figures like Marconi, Franklin, and Munk contributing to the theoretical and practical foundations. The emphasis on tuning elements and understanding resonant frequencies has since become central to the design and optimization of periodic surfaces for various applications, including but not limited to military uses.

1.3. Different types of Periodic Array

1.3.1. Dipole Array

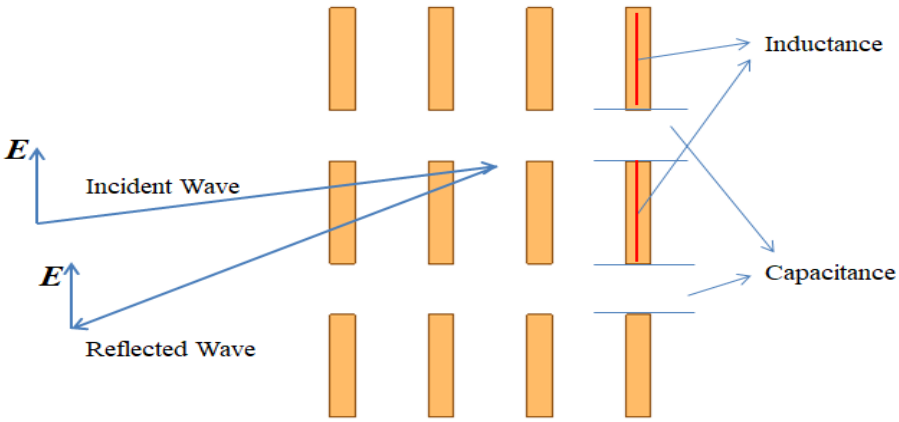

Fig. 1.1.2. Dipole array.

A dipole array is composed of metal strips arranged in a periodic fashion (Fig. 1.1.2.). When an electromagnetic wave interacts with this structure and the incoming electric field aligns parallel to the conducting strips, a series of interesting phenomena occur. The behavior is particularly significant when the dimensions of the strip are such that resonance is achieved, typically when the length of the strip is approximately half of the wavelength of the incident wave.

In a periodic structure, when resonance is achieved at this specific frequency, the radiated energy from the oscillating electrons in the conducting strip adds in phase with

the incoming wave. Simultaneously, it opposes the transmitted wave. As a result, at the resonant frequency, the incident wave experiences complete reflection, and the structure effectively functions as a band-stop filter for incoming electromagnetic waves.

At the resonant frequency, the dipole array behaves like a series LC (inductance-capacitance) circuit. The periodic arrangement of metal strips reinforcing the reflected wave and attenuating the transmitted wave. This phenomenon is exploited in the design of various devices, such as filters, where the dipole array serves as an effective means to block specific frequencies. Understanding and manipulating these resonant characteristics are crucial for optimizing the performance of dipole arrays.

1.3.2. Slot Array

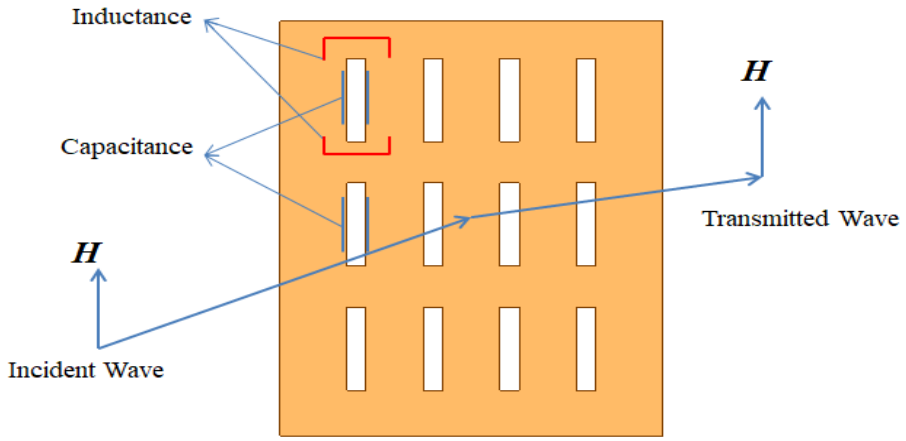

Fig. 1.1.3. Slot array.

A slot array is a structure that consists of periodically etched slots on a metal sheet (Fig. 1.1.3.). When an electromagnetic wave impinges upon one of these slots, it induces a voltage in the slot. The induced voltage can be understood and analyzed using the field equivalence principle, which allows this induced voltage to be represented by a fictitious magnetic current. This representation aligns with the concept of duality in electromagnetic theory. Babinet's principle states that the slot in the conducting surface

is dual to a simple conducting strip. In other words, the behavior of a slot in a metal sheet is similar to that of an open region in the same metal sheet.

As a result of this dual behavior, the slot array functions as a band-pass filter for incident electromagnetic waves at a particular frequency. The resonance of the structure occurs when the length of the slot is approximately half of the wavelength of the incident wave. This resonance condition is critical in determining the frequency response of the slot array. At the resonant frequency, the structure acts like a parallel LC (inductance-capacitance) circuit. This phenomenon allows the slot array to selectively pass and enhance electromagnetic waves at the specific frequency determined by the dimensions of the slots.

1.4. Complementary Arrays

Complementary arrays refer to a combination of dipole arrays and slot arrays that share similar-shaped elements. Specifically, the term "complementary" here implies that the geometrical shapes of the elements in the dipole array and slot array are designed to complement each other. When these two types of arrays are superimposed or combined, they collectively form a complete, perfectly conducting plane. In this context, the specular reflection coefficient for one of the arrays is essentially equivalent to the transmission coefficient for the complementary array.

The concept of complementary arrays finds applications in antenna design, electromagnetic shielding, and other areas where control over the reflection and transmission of electromagnetic waves is crucial. By carefully designing the shapes and arrangements of dipole and slot elements, engineers can tailor the properties of these complementary arrays to achieve specific electromagnetic responses in a variety of practical scenarios.

1.5. Resonant Behaviour of the FSS Elements

The fundamental characteristics and frequency response of typical elemental components utilized in the design of FSS are elucidated in [1]. The elements interconnected at their center exhibit resonance when their longest tip-to-tip dimension is approximately equal to half the wavelength, while loop-type elements resonate when their average circumference is approximately one wavelength.

The bandwidth of FSS primarily relies on the spacing between individual elements. Additionally, introducing a thin dielectric layer will slightly reduce the resonant frequency for both dipole and slot arrays. Furthermore, by cascading two or more arrays, a band-pass filter characteristic with a flat top and a steep roll-off can be achieved.

When an electromagnetic wave encounters a FSS and approaches it at a particular angle relative to the normal of the FSS plane, two phenomena typically take place: transmission and specular reflection, occurring at the same angle of incidence. However, there exists a specific frequency range where, rather than experiencing transmission and specular reflection, the wave undergoes a unique behavior. In this range, the wave is reflected at an angle different from the incidence angle, aligning itself with the original direction of the incident wave.

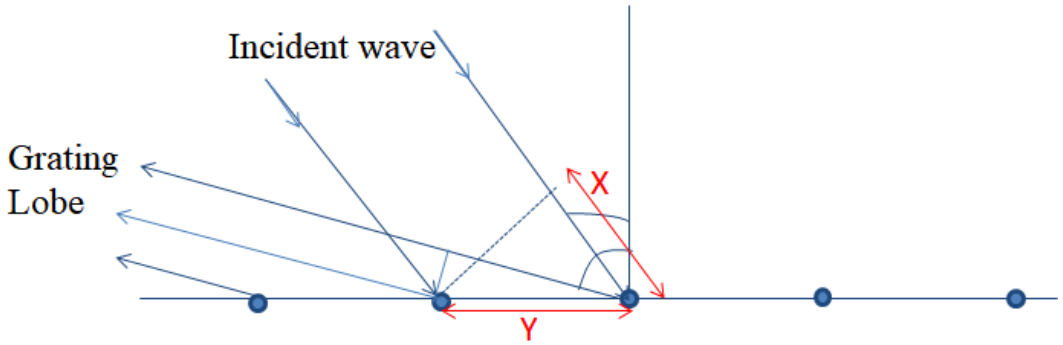

Fig. 1.2. Grating Lobe.

If the phase difference experienced by the wave when traveling distances X and Y (as shown in the figure) is equal to zero, then a grating lobe occurs (Fig.1.2).

This peculiar reflection phenomenon exhibited by the FSS is denoted as a grating lobe. The term "grating lobe" signifies an unintended secondary direction of the reflected wave, distinct from the expected transmission and specular reflection patterns. The frequency at which the grating lobe occurs is contingent upon two primary factors: the angle of incidence and, significantly, the distance between individual unit cells within the FSS structure. The interplay of these factors determines the appearance and behavior of grating lobes, contributing to the intricate response of the FSS to incident waves within the specified frequency range.

1.6. Analysis of FSS

The assessment of periodic configurations and the methodology for ascertaining the scattering and impedance characteristics of FSS structures is given in [1].

The text outlines the steps involved in understanding the behavior of the FSS when subjected to electromagnetic waves.

Induction of Current: When an electromagnetic wave hits the FSS element, it induces a current within the structure.

Calculation of Magnetic Vector Potential and Magnetic Field: The induced current allows for the determination of the magnetic vector potential and magnetic field at a certain distance from the FSS element.

Computation of Electric Field: Using the magnetic field information, the electric field is computed.

Transmission and Reflection Coefficients: With the electric field and magnetic field data, the transmission and reflection coefficients of the FSS element are

determined. These coefficients provide insights into how much of the incident wave is transmitted through and how much is reflected by the FSS element.

Floquet Theorem-Based Periodic Boundary Conditions: To analyze the response of the entire periodic structure, Floquet theorem-based periodic boundary conditions are applied along the unit cell of the FSS. The Floquet theorem states that, an infinite, planar, periodic structure illuminated by an infinite plane wave, each unit-cell of the periodic structure exhibits identical currents and fields, with only a phase shift corresponding to the incident field phase.

Numerical Techniques for Analysis: Various numerical techniques have been developed to analyze periodic structures with periodic boundary conditions. Examples include:

Finite Element Method (FEM)

Method of Moments (MoM)

Finite-Difference Time-Domain (FDTD)

These numerical methods are employed to solve partial differential equations, providing a computational framework to simulate and understand the electromagnetic behavior of the FSS element and the overall periodic structure. The goal is to gain insights into how these structures interact with electromagnetic waves, aiding in the design and optimization of devices for specific applications.

1.7. Applications of FSS

The significant applications of FSS are discussed below.

1.7.1. Electromagnetic Shielding and Interference Reduction

FSS can be employed as electromagnetic shielding to control the propagation of electromagnetic waves based on their frequency. The primary goal of using FSS for electromagnetic shielding is to selectively block or allow specific frequency bands, providing a tailored and effective means of shielding against electromagnetic interference.

- FSS can be integrated into wireless communication devices, such as smartphones and routers, to improve signal reception and filter out interference from other electronic devices operating at nearby frequencies.
- FSS materials are employed in aerospace applications for electromagnetic interference shielding, which is critical for the proper functioning of avionics and communication systems in aircraft and spacecraft.
- FSS are used in satellite communication systems to control the transmission and reception of signals at different frequencies. They can be employed as filters and beam-steering devices on satellite antennas.
- FSS can be incorporated into radar systems and remote sensing to create specialized frequency-selective surfaces that enhance radar performance by allowing certain frequencies to pass through while blocking others.
- FSS are used in automotive radar systems for collision avoidance and adaptive cruise control. They help in shaping the radar beams and reducing interference.
- In medical imaging, FSS can be used as shielding materials to control electromagnetic interference and improve the performance of imaging equipment like MRI machines and CT scanners.

- FSS can help enhance the range and accuracy of RFID systems by controlling the propagation of RFID signals, improving read rates, and reducing interference.
- FSS technology can be used in security systems, such as perimeter protection and border control, to enhance the performance of surveillance and sensing equipment.

1.7.2. Radome Design

A radome is a protective structure, often in the form of a dome or other shape, shielding radar equipment. These structures are crafted from materials transparent to radio waves, particularly when situated on the outer surface of spacecraft, aircraft, or missiles. When designed using FSS, the radome selectively allows only desired frequencies to pass through, while scattering or blocking all other frequencies. This unique property makes FSS-based radomes invaluable in stealth applications, where the controlled transmission and reception of specific frequencies are critical for minimizing the radar signature and enhancing overall stealth capabilities.

1.7.3. Wave Polarizers

The geometry and orientation of the conductive elements in the FSS can be tailored to be sensitive to the polarization of incident electromagnetic waves. Polarization refers to the orientation of the electric field vector in an electromagnetic wave, and FSS can be designed to interact differently with waves of different polarizations. Depending on the design, FSS can selectively pass or block specific polarizations of electromagnetic waves. This is achieved by configuring the conductive elements to have different responses to waves with varying polarization states. FSS can be engineered to rotate, convert, or otherwise manipulate the polarization state of

incident waves. This capability is particularly useful in applications where control over the polarization of transmitted or received signals is essential.

FSS polarizers find applications in antennas and communication systems where precise control over the polarization of transmitted or received signals is required. By incorporating FSS into the design, it becomes possible to enhance the performance of antennas and communication systems by tailoring them to specific polarization requirements.

1.7.4. FSS Absorber

The conventional Salisbury screen (Fig.1.3 (a)) comprises a resistive sheet positioned one-quarter wavelength in front of a ground plane. To avoid ambiguity caused by objects behind the absorber sheets, all absorbers typically incorporate a ground plane. Named after its inventor, W.W. Salisbury of the MIT Radiation Laboratory, this absorber design received a patent in 1952. A variant, known as the Jaumann absorber (Fig.1.3 (b)), closely resembles the Salisbury screen but utilizes two or more homogeneous resistive sheets in front of a ground plane.

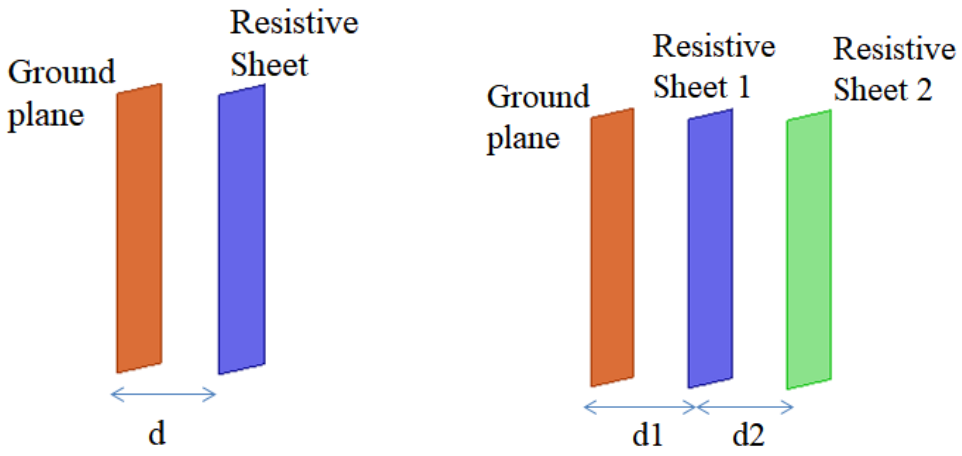

(a) (b)

Fig. 1.3. (a) Salisbury screen (b) Jaumann absorber.

Both the Salisbury screen and the Jaumann absorber employ purely resistive sheets [1]. In contrast, circuit analog absorbers introduce a new dimension by utilizing sheets that are not only resistive but also reactive. This is achieved through the use of periodic surfaces (FSS) made of lossy material. The resistive component arises from the lossy element material, while inductance is associated with the straight parts of the conducting elements, and capacitance is linked to the gaps between the conducting elements.

FSS play a pivotal role in military applications, especially in stealth technology. By creating radar-absorbing materials (RAMs), FSS effectively reduce the radar cross-section (RCS) of aircraft, ships, and ground vehicles. This technological advancement renders these platforms virtually undetectable by radar systems, making FSS a crucial element in enhancing stealth capabilities.

1.7.5. Transmitarray

The primary function of the FSS in a transmitarray is to control the phase of the transmitted waves. By manipulating the geometry and dimensions of the FSS elements, the phase of the transmitted waves passing through each unit cell can be adjusted. The FSS allows the transmitarray to be frequency-selective. It can be engineered to exhibit different transmission properties at various frequencies, enabling the control of electromagnetic waves within a specific frequency band. The phase adjustments introduced by the FSS in each unit cell allow for precise control of the direction in which the transmitted beam is steered. By adjusting the phase across the transmitarray, the overall direction of the transmitted beam can be manipulated.

1.7.6. Reflectarray

The function of the reflectarray is same as that of the transmitarray. Transmitarray manipulate the phase of transmitted waves, while reflectarray manipulate the phase of reflected waves.

1.8. Literature Review

Over the past few years, there has been a surge in research devoted to FSS due to their extensive applications in defense, space technology, and the commercial sector. Researchers have well-demonstrated the use of FSS for various applications such as electromagnetic shielding [2-7], stealth radomes [8-13], wave polarizers[14-18], absorbers[19-24], transmitarray [25-30], reflectarray [31-35], remote sensing[36-38], and many other applications. The literature survey conducted using some examples of the different structures of FSS.

1.8.1. Basic Elements

The resonant behaviour of the some basic elements such as dipole, tripole, Jerusalem cross, square spiral, loop type, three and four legged loop, and hexagon elements are clearly explained by Munk in [1]. A favorable characteristic is the ability to maintain a consistent resonance response when subjected to changes in incident angles. Various loop configurations, including three and four-legged loaded elements, as well as simple circular and square loops, along with hexagonal elements, prove beneficial for applications requiring broad frequency coverage. Some basic element FSS designs reported in the literature are discussed.

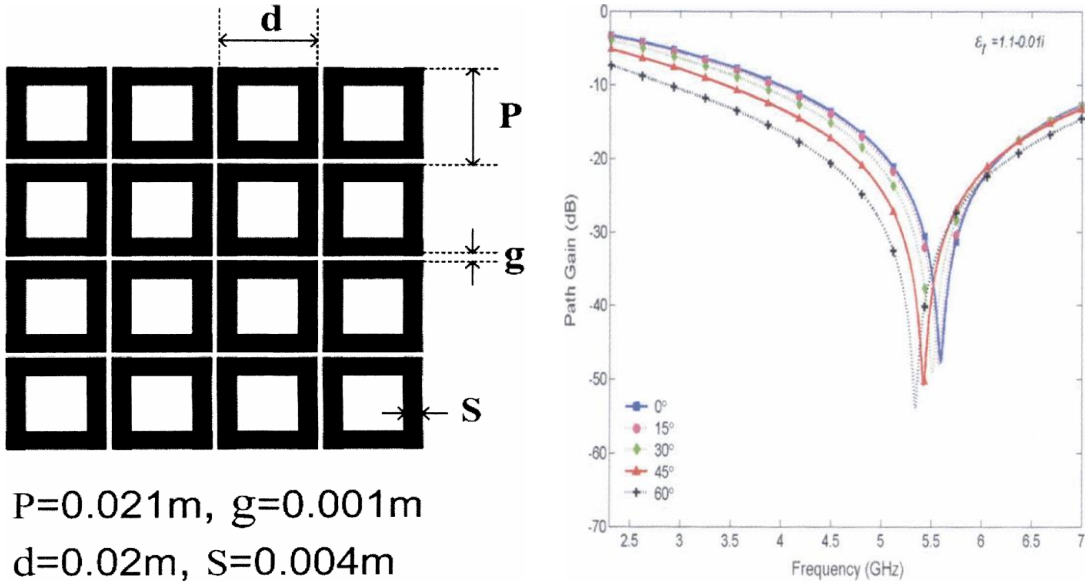

Fig. 1.4. Square loop bandstop FSS proposed by [39] and its response.

FSS using square loop structure (Fig. 1.4.) was designed to reduce interference in indoor wireless environments [39], a standard office partition wall positioned in the primary propagation path underwent a conversion into a frequency-selective (FS) wall. This transformation involved affixing a specially designed band-stop FSS as a covering on the wall surface. On-site measurements revealed that this frequency-selective wall effectively screened signals operating within the 5.4-6.0 GHz range (IEEE 802.11a), providing an extra attenuation of 10-15 dB compared to the unaltered wall, across incident angles spanning from 0 to 55 degrees.

Literature [40] introduces a FSS design tailored for applications in Wi-Fi shielding, serving as a band-reject dual-band single-layer filter. The proposed design integrates fundamental elements, specifically ring loops, and is calibrated to operate efficiently at both 2.4 and 5.2 GHz Wi-Fi frequency bands (Fig. 1.5). The design exhibits a consistently stable frequency response within the mentioned Wi-Fi bands, accommodating incidence angles spanning from 0° to 45°.

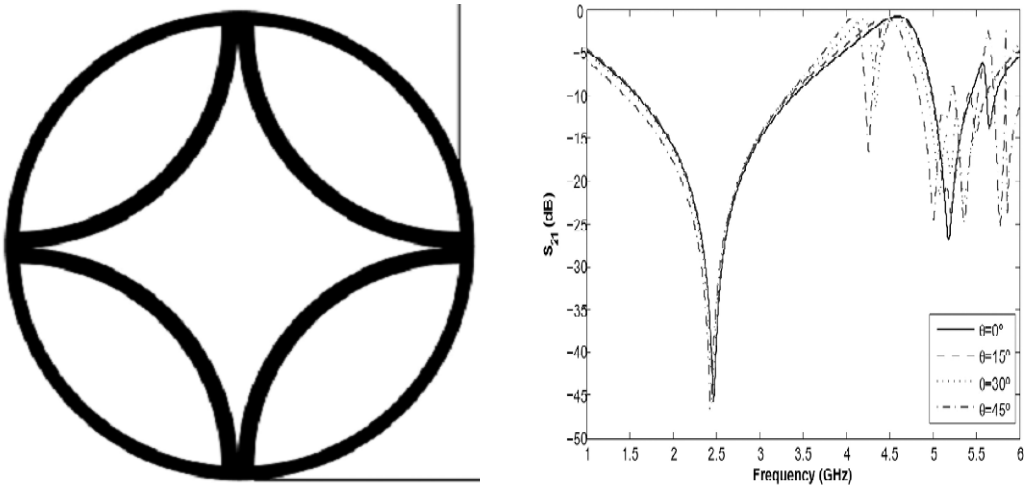

Fig. 1.5. Circular loop type bandstop FSS proposed by [40] and its response.

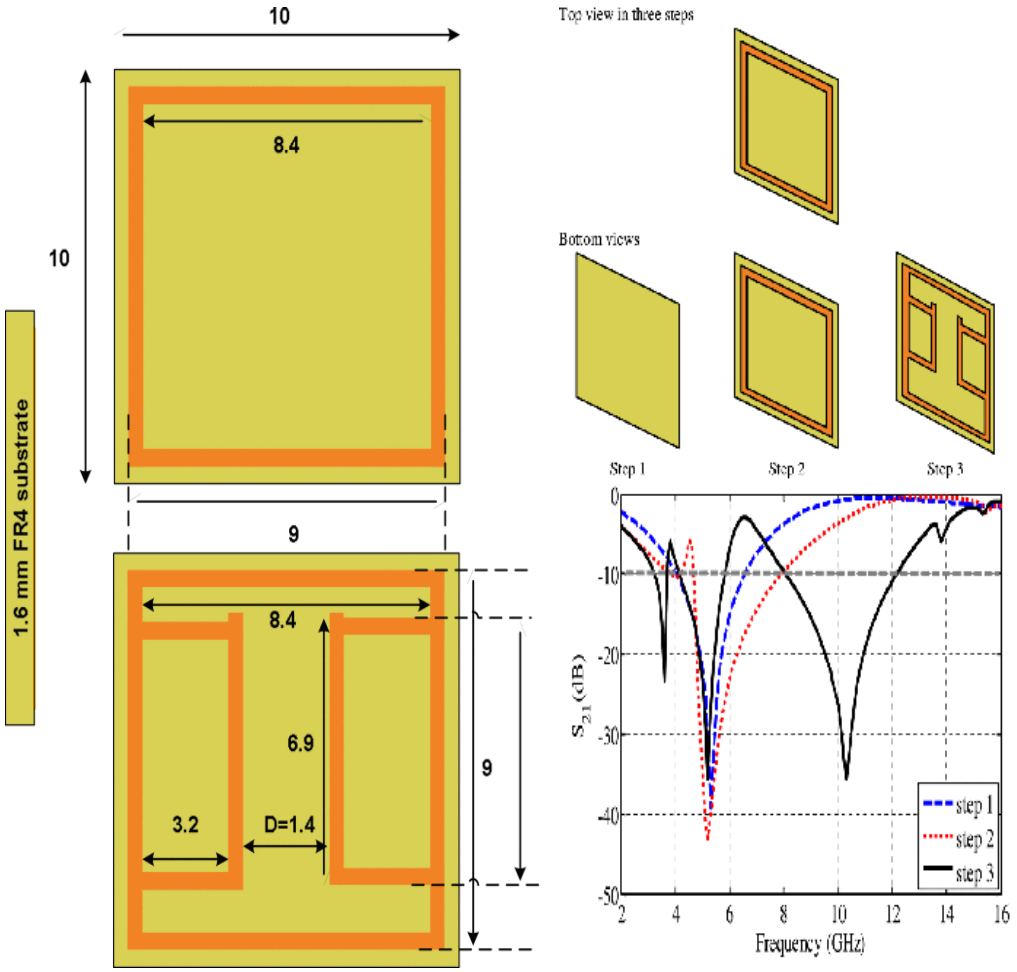

Fig. 1.6. Proposed FSS [41] for WiMAX, WLAN, and X-band filtering.

A single-substrate-layer FSS [41] is proposed for triple-band-stop filtering applications. The design incorporates straightforward conductive elements on both sides

of the substrate (1.6 mm thick FR4). On the top side, a square loop is positioned, while on the backside, another square loop combined with two folded arms is embedded (Fig. 1.6). The integration of these conductive elements, with carefully chosen dimensions, enables the FSS to operate across three distinct frequency bands: 3.2-3.7, 4.1-6, and 8-12.1 GHz, covering WiMAX, WLAN, and X-band within the specified frequency ranges, respectively. As a key performance metric, the presented band-stop FSS structure demonstrates a stable frequency response against varying angles of TE and TM polarizations.

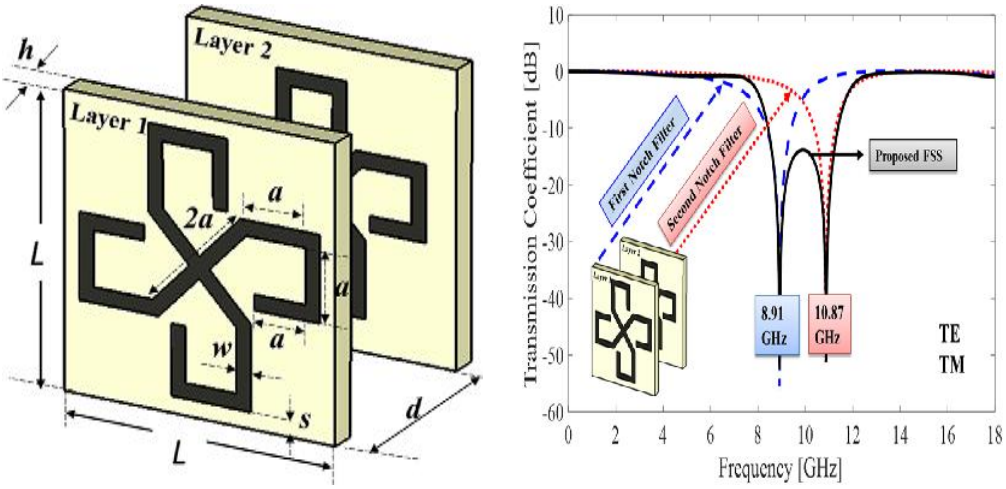

Fig. 1.7. Proposed FSS [42] for broadband and X-Band application.

A higher-order miniaturized band-stop FSS [42] designed for optimal performance in X-band applications. The miniaturization is achieved by curving the arms of the conventional cross-dipole shape inwards (Fig. 1.7). The unit cell size of the FSS is reduced by up to 75% when compared to a cross-dipole FSS operating at the same resonant frequencies. The presented FSS maintain stable angular performance, accommodating incident angles up to approximately 60° for both TE- and TM-polarized waves. By cascading the similar type of structures broadband response has been achieved in this literature. It is the advantage over the single layer structure, which gives narrow band response.

A novel FSS for millimeter-wave applications is introduced in [37], aiming to demultiplex four atmospheric remote sensing bands characterized by varying bandwidth (3-20 GHz) and frequency separation (50-195 GHz). The unit cell, measuring 670 μm × 670 μm, comprises a circular metal mesh loaded with a monopole integrated concentric ring on a 175-μm-thick quartz substrate (Figure 1.8: dx = 670 μm, dy = 670 μm, w = 20 μm, w_1 = 20 μm, r_1 = 280 μm, r_2 = 260 μm, g = 100 μm. Gray (white) portion is gold (quartz)). This design is tailored to reject frequencies within the ranges of 50-60 GHz (B1), 87-91 GHz (B2), and 148-151 GHz (B3), while facilitating transmission in the range of 175-195 GHz (B4). The FSS is optimized for both transverse electric (TE) and transverse magnetic (TM) polarizations under oblique incidence angles ranging from 25° to 35°.

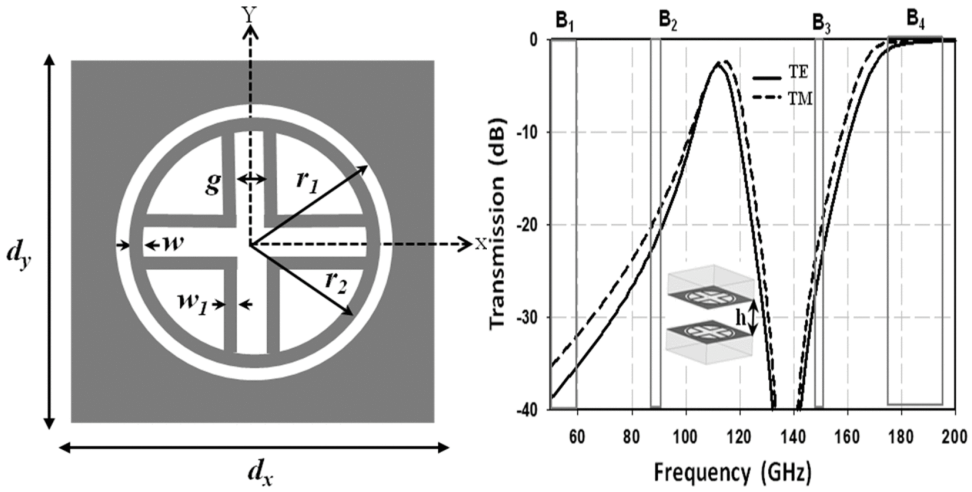

Fig. 1.8. Unit cell of the quad-band FSS [37] and its response.

[43] introduced a single-layer FSS designed for superior angular stability. The proposal involves creating a combined FSS (CFSS) element by integrating two modified cross loops (Fig. 1.9). The CFSS, owing to its rotationally symmetrical structure, exhibits insensitivity to the incidence of TE or TM polarizations (Fig.1.10). Through this combination, the FSS achieves a notable angular stability property, with a

maximum resonant frequency deviation of only 0.08 GHz over incident angles ranging from 0° to 85°.

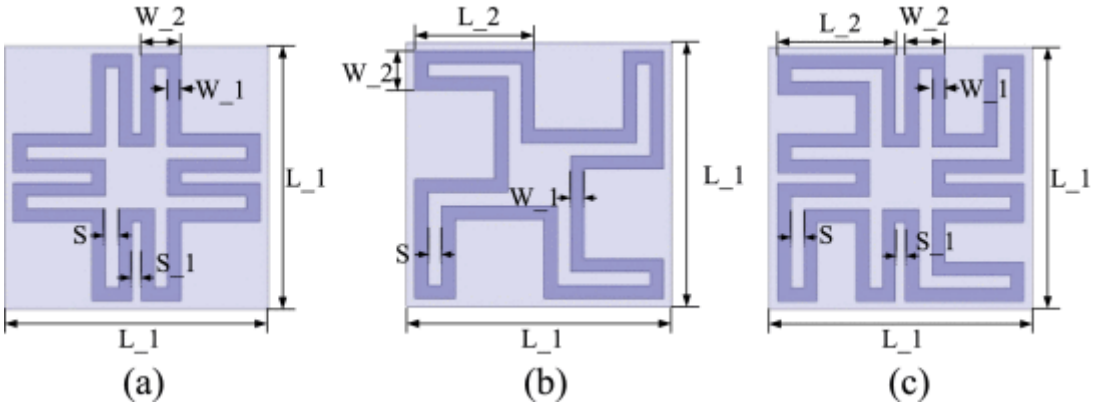

Fig. 1.9. Proposed FSS [43] (a) Double-arc axisymmetric cross loop (DACL), (b) Single-arc centrosymmetric cross loop (SCCL), (c) Combined FSS.

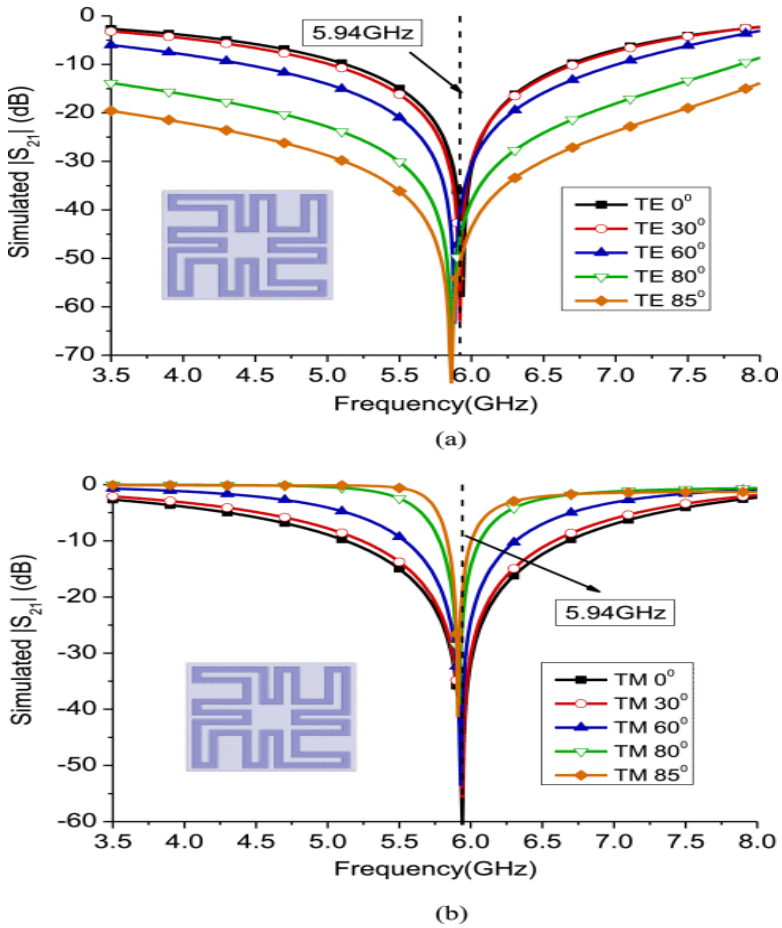

Fig. 1.10. Simulation results of proposed FSS in [43] (a) TE (b) TM polarizations.

Sarabandi and Behdad introduced a new class of bandpass FSS [44]. The proposed FSS is composed of a periodic array of metallic patches separated by thin air-gaps, backed by a wire mesh with the same periodicity (Fig. 1.11). Within this configuration, the metallic patches form a capacitive surface, while the wire mesh serves as a coupled inductive surface. Together, these components create a resonant structure intercepting incident plane waves. Similar to traditional FSSs, the capacitive and inductive surfaces of the proposed FSS can be easily fabricated using printed circuit technology on both sides of microwave substrates. The researchers demonstrated that by cascading such bandpass surfaces in a specific manner, it is possible to achieve arbitrary multipole filters or non-commensurate multiband responses.

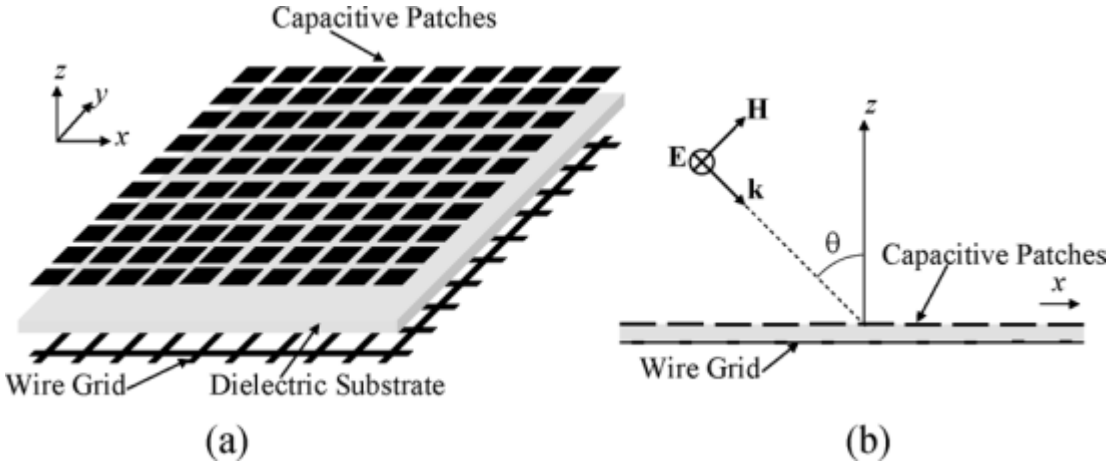

Fig. 1.11. Proposed FSS by Sarabandi and Behdad [44].

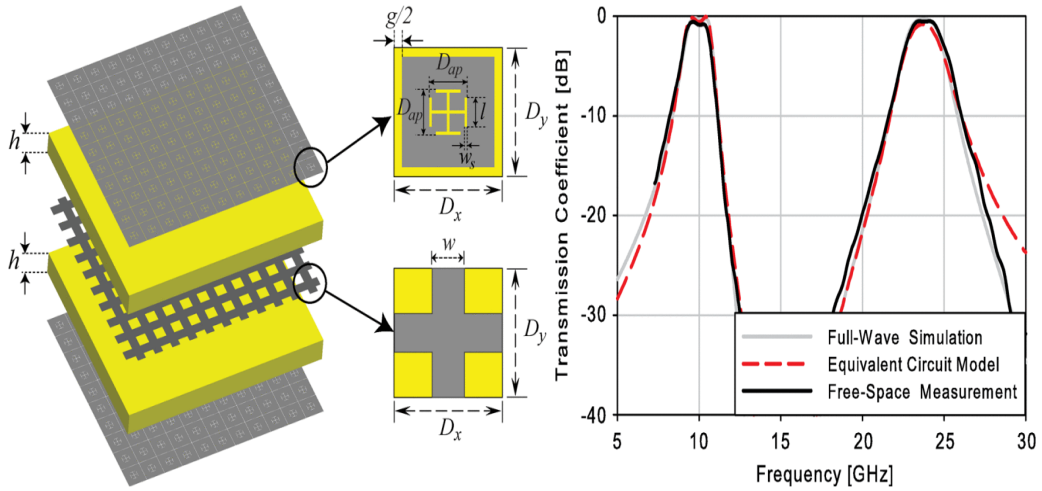

Fig. 1.12. Proposed FSS in [45].

A band-pass FSS of second-order is outlined in reference [45]. The design comprises three conductive layers, with the first and third layers being identical and incorporating Jerusalem crosses embedded in sub-wavelength capacitive patches (Fig. 1.12). The second layer is characterized by an inductive grid. This structure functions as a band-pass FSS, operating effectively in both X- and Ka-bands.

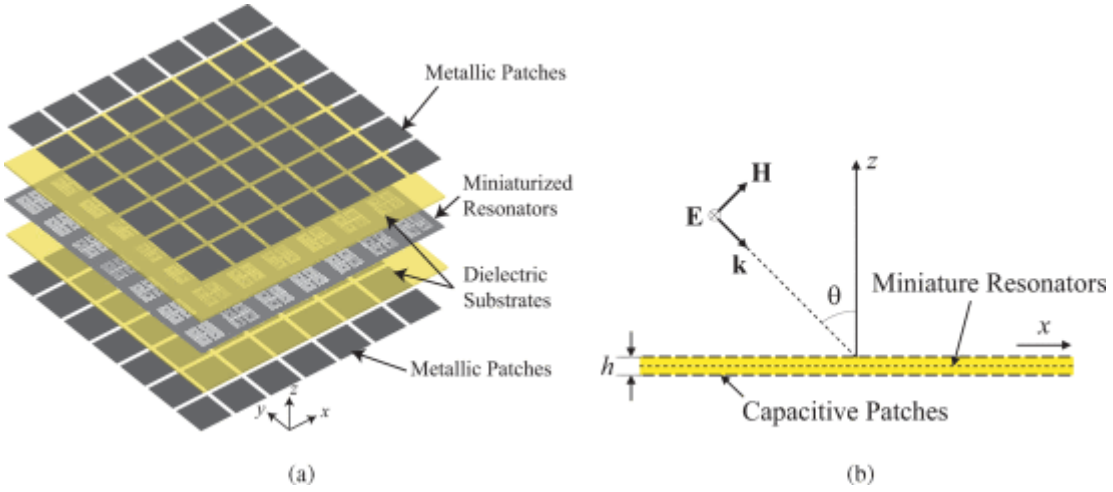

Fig. 1.13. Proposed FSS in [46] (a) 3 –D view (b) side view.

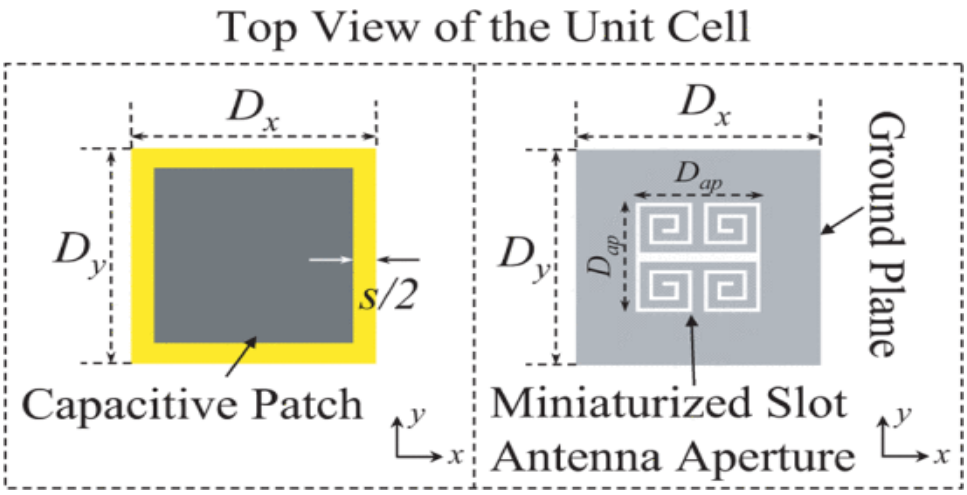

Fig. 1.14. Top view of the unit-cell [46].

The proposed FSS [46] constitutes a three-layer structure comprised of three metal layers, each separated by thin dielectric substrates. Each layer exhibits a two-dimensional periodic structure with unit cell dimensions and periodicity that are sub-wavelength (Fig. 1.13 & Fig. 1.14). The unit cell of this proposed FSS is crafted by

combining resonant and non-resonant elements. It has been demonstrated that this configuration serves as a spatial bandpass filter, displaying a third-order bandpass response (Fig. 1.15).

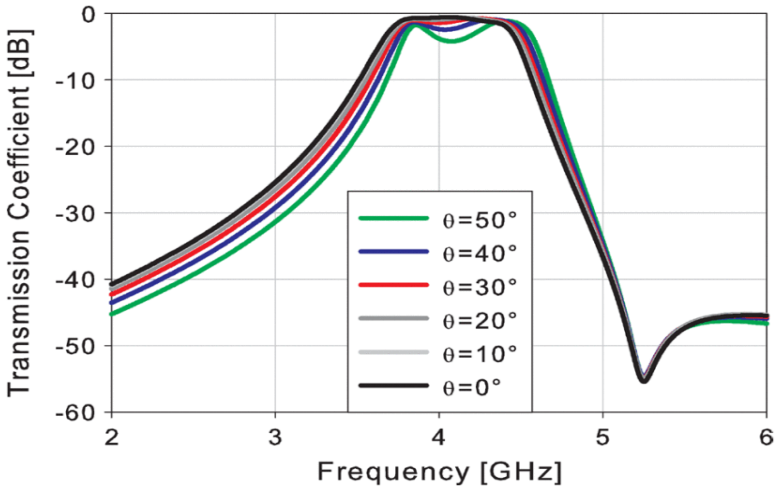

Fig. 1.15. Transmission coefficients of the FSS proposed in [46].

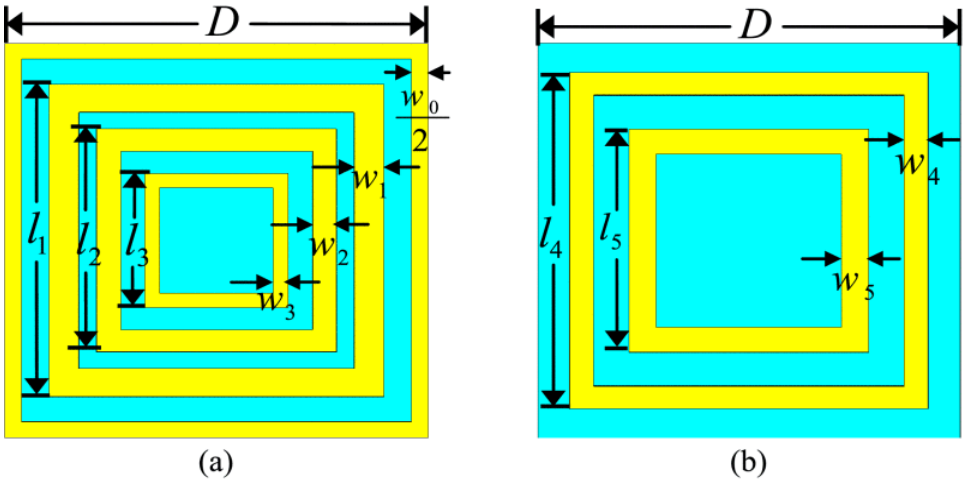

Fig. 1.16. Proposed FSS structure in [47].

In reference [47], a quad-bandpass Frequency-Selective Surface (FSS) is created by stacking three metallic layers, each separated by two thin dielectric substrates (Fig. 1.16.). The outer layers are constructed as periodic arrays of gridded-triple square loops (G-TSLs), while the middle layer features an array of double square loops (DSLs). Fig. 1.17 the frequency of the structure.

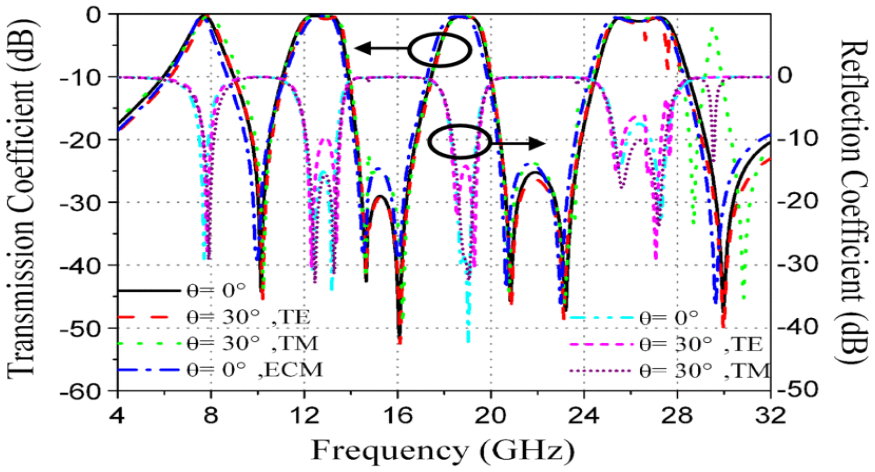

Fig. 1.17. Frequency response of proposed FSS structure in [47].

A new design for a polarization rotator presented in [17], based on Frequency-Selective Surface (FSS). This polarization rotator selectively permits the transmission of linearly polarized incident waves through the structure and induces a 90° rotation within a specified frequency band. The periodic element in the FSS design comprises V-shaped slots oriented orthogonally on two metal sheets, with a dielectric substrate positioned between them (Fig. 1.18.).

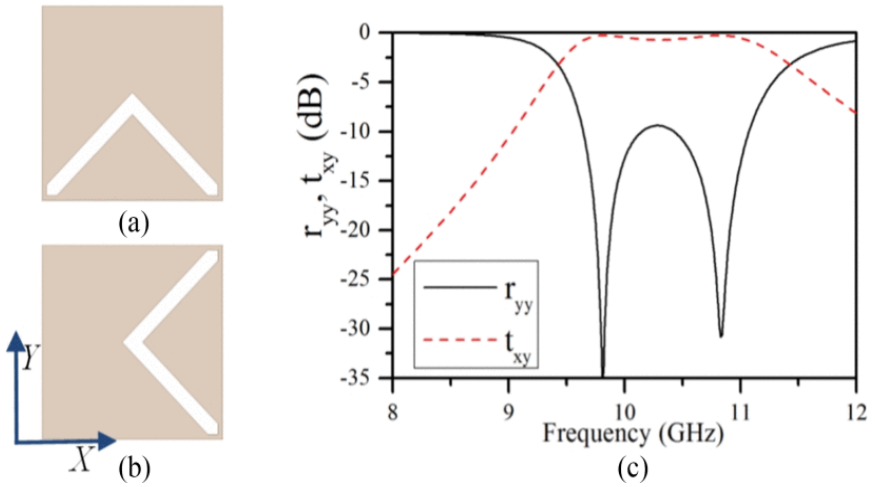

Fig. 1.18. (a), (b) proposed FSS structure in [17], (c) its response.

A novel FSS is introduced in [48], designed to exhibit low cross-polarization with minimal passband ripples and a sharp roll-off on either side of the passband. Diverging from existing substrate integrated waveguide FSSs, where every unit cell

boundary is electrically conducting, the proposed FSS unit cell is constructed with two specially designed cavities featuring mixed electrically and magnetically conducting boundaries (Fig. 1.19.). These boundaries are created through an array of shorting vias and complementary slots, etched on the top and bottom metallic patches, respectively. Fig. 1.20. shows the frequency response of the structure.

The suggested FSS [10] configuration comprises two layers embedded within five dielectric substrates, making it well-suited for constructing FSS radomes (Fig. 1.21). The upper FSS layer incorporates gridded square loop elements, while the lower layer features cross-loop aperture elements. These two FSS layers are segregated by a core material layer designed for coupling. Additionally, skin material and foam material layers are affixed externally to the FSS layers to facilitate bandwidth compensation. Fig. 1.22 shows the response of this structure.

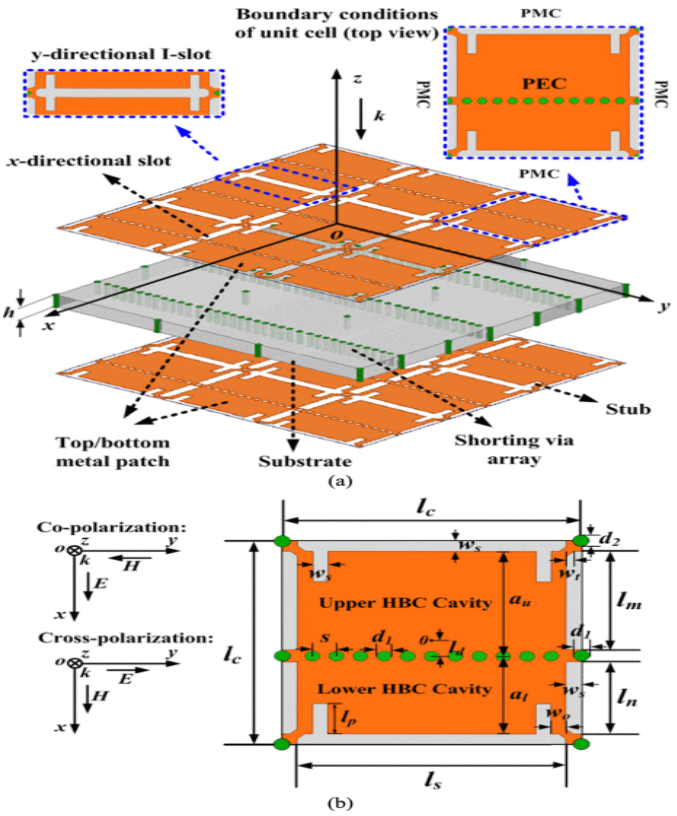

Fig. 1.19. (a), (b) proposed FSS structure in [48].

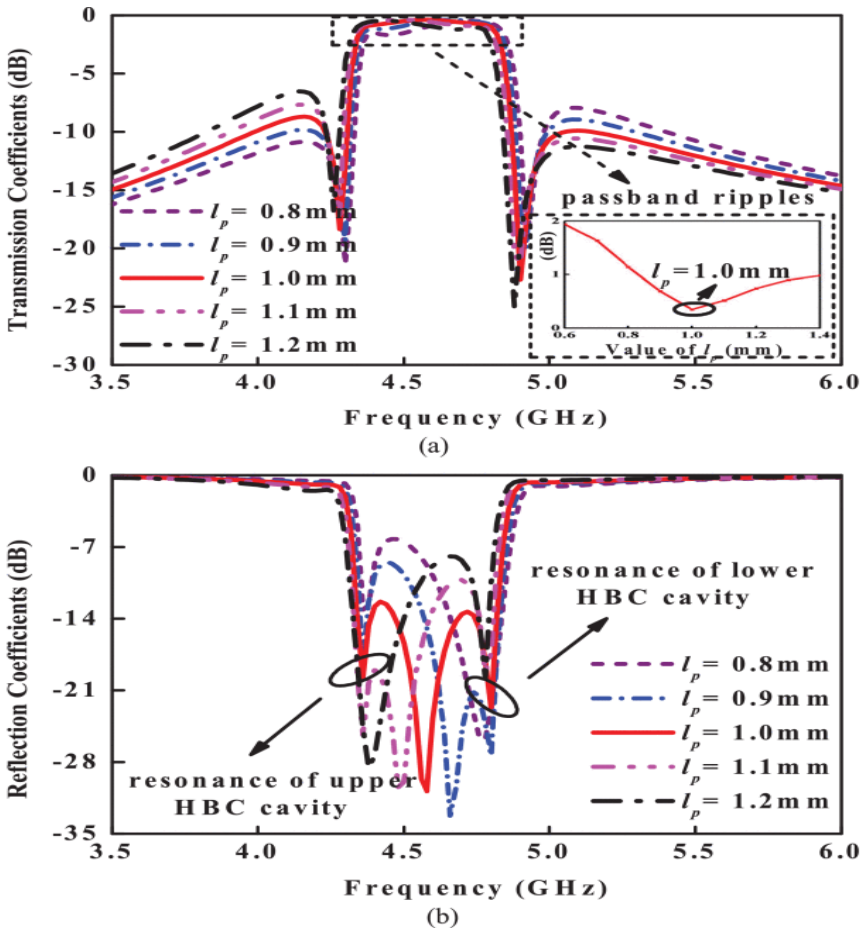

Fig. 1.20. (a) Transmission and (b) reflection coefficient of the structure proposed FSS structure in [48].

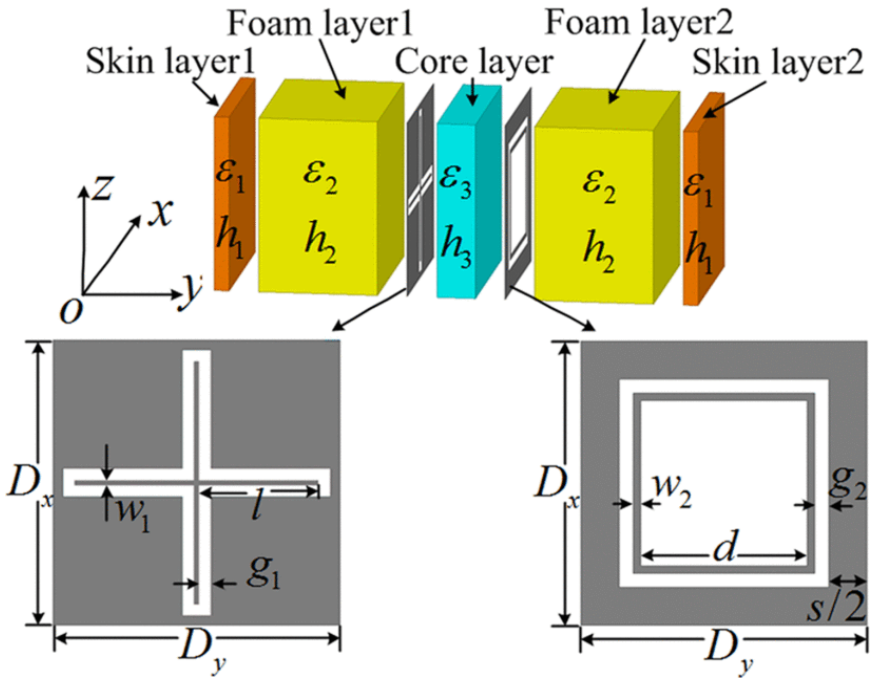

Fig. 1.21. (a), (b) proposed FSS structure in [10].

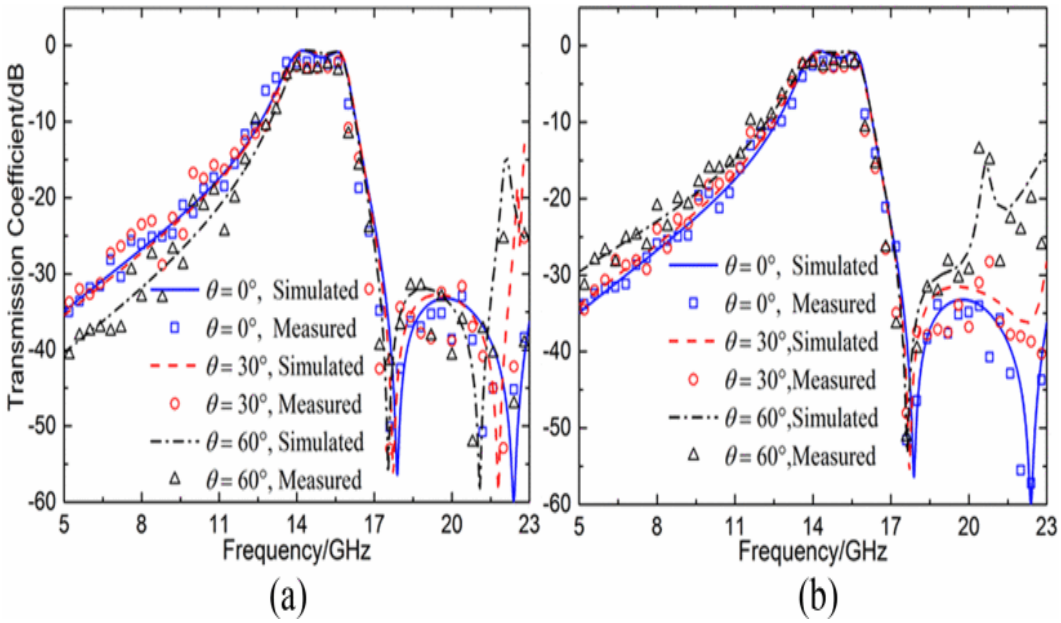

Fig. 1.22. Simulated and measured results of the proposed FSS structure in [10] (a) TE (b) TM polarizations.

1.8.2. Meandered or Convoluted Structures

A closely spaced dual-band angularly stable FSS reported in [49]. The single-layer FSS proposed in this study consists of unit cells designed in a crooked cross geometry, intricately convoluted and branched to create dual resonant paths (Fig. 1.23). Operating as a band stop filter at 2.54 and 3.54 GHz, serves as an effective shielding element for these frequencies.

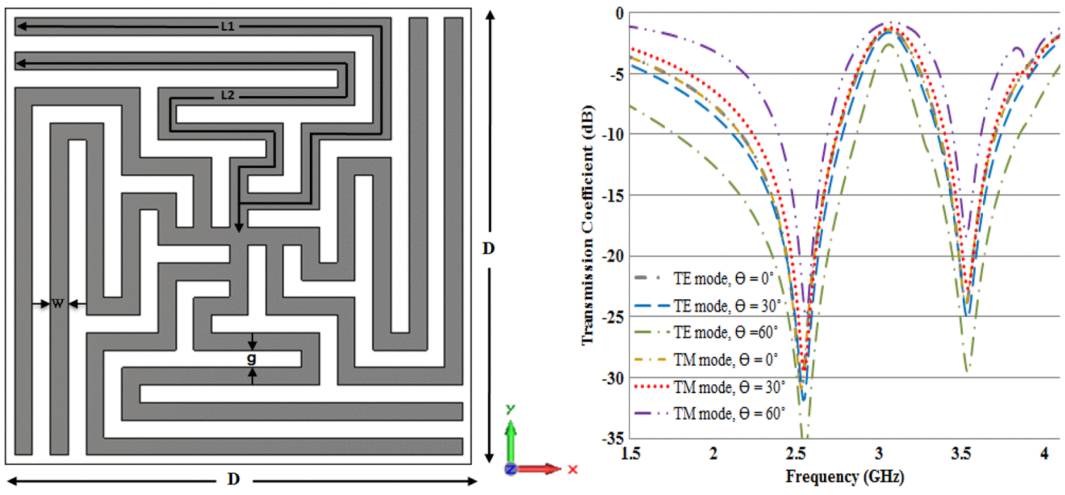

Fig. 1.23. Proposed convoluted FSS structure in [49] and its frequency response.

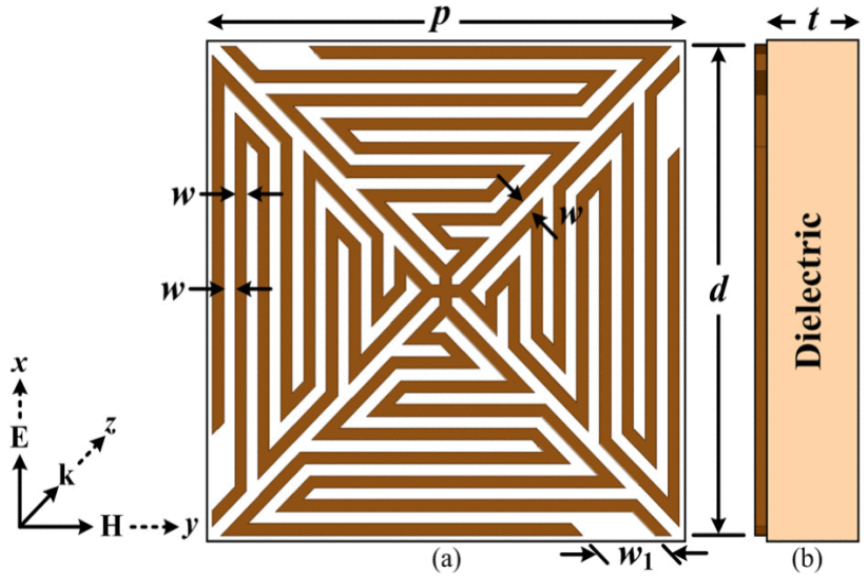

Fig. 1.24. Unit cell geometry of the proposed dual-band meandered FSS in [50]. (a) Top view. (b) Side view.

The reported FSS in [50] is constructed with meander lines printed on a single-layer dielectric substrate, yielding dual stopband characteristics (Fig. 1.24). This FSS design exhibits improved miniaturization properties. Additionally, the proposed structure remains polarization-independent and maintains angular stability for both TE and TM polarizations (Fig. 1.25).

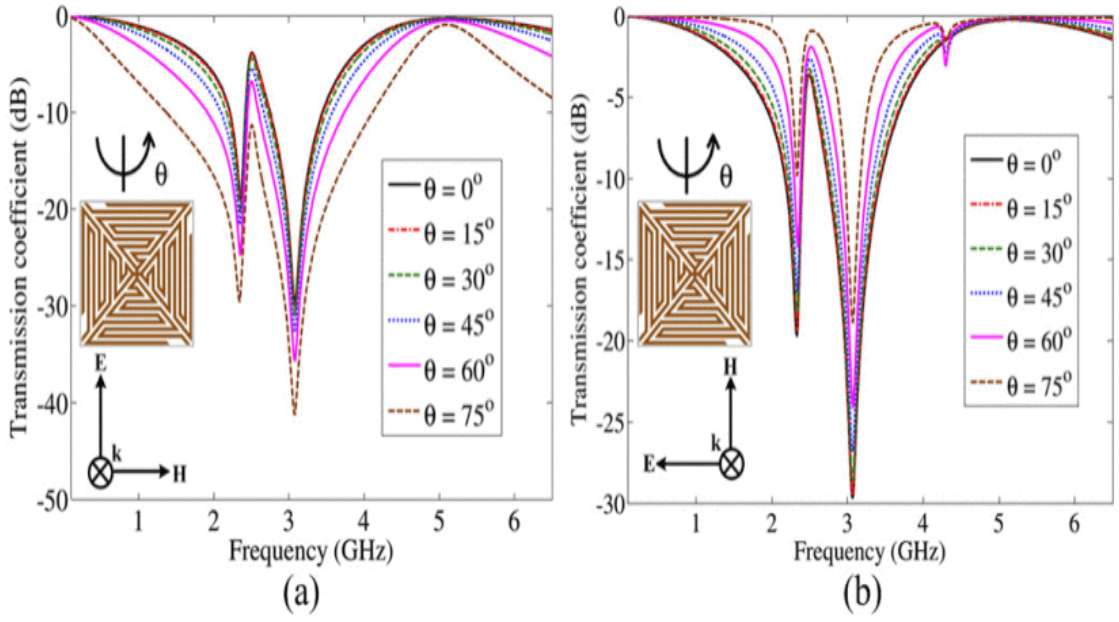

Fig. 1.25. Simulated results of the proposed FSS in [50] (a) TE (b) TM polaizations.

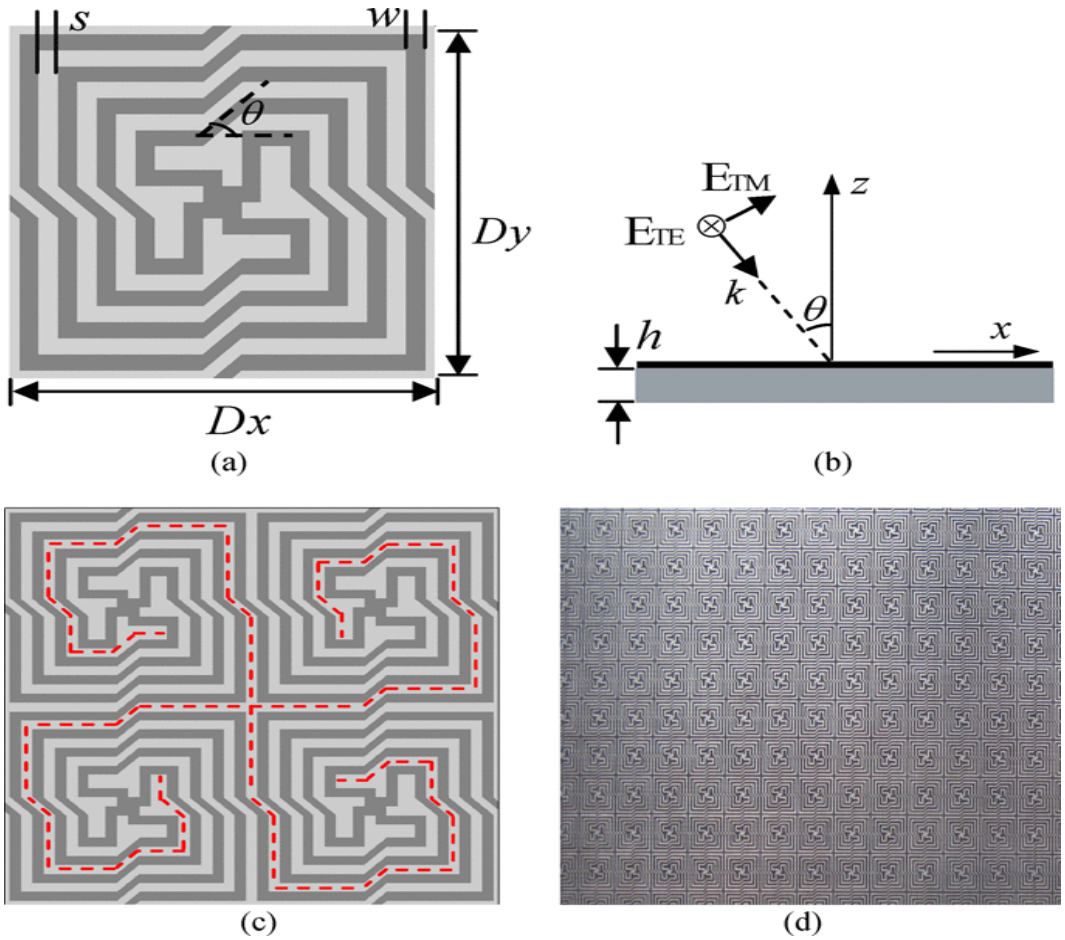

Fig. 1.26. Proposed bandpass FSS in [51] (a) Front view of the unit cell. (b) Side view of the unit cell. (c) 2×2 unit cells. (d) Prototype of the FSS.

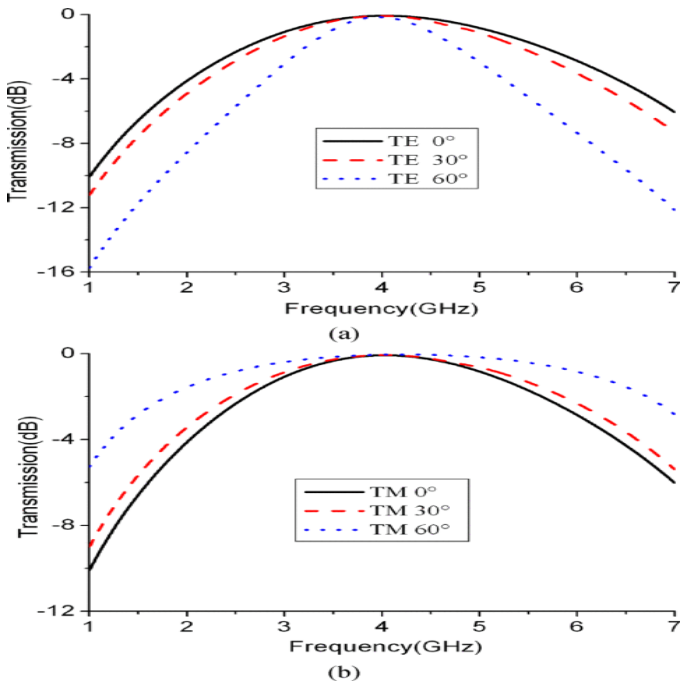

Fig. 1.27. Simulated results FSS proposed in [51].

A bandpass FSS documented in [51], featuring miniaturized periodic elements (Fig. 1.26). The FSS design is printed on a single-layer substrate with a relative permittivity of 2.65. The simulated results of this structure are shown in Fig. 1.27.

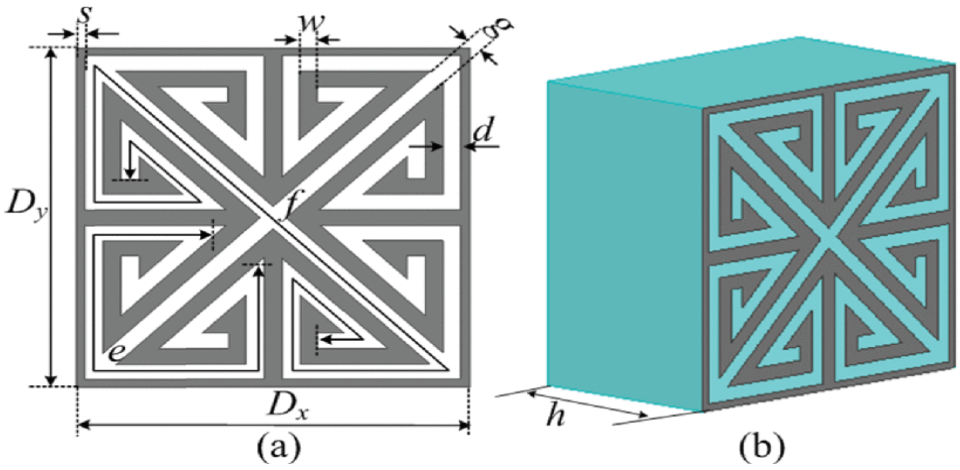

Fig. 1.28. Reported FSS structure in [52], (a) top view (b) side view.

The proposed FSS [52] is comprised of a cross-dipole aperture element in conjunction with a meandered monopole aperture element (Fig. 1.28). This single-layer FSS offers two pass-bands centered at 5.13 and 8.85 GHz (Fig. 1.29). The pass-band frequencies can be independently controlled by adjusting the structural parameters of the unit cell. Additionally, the designed dual-band FSS, utilizing miniaturized elements, exhibits good resonance stability for various polarizations and incident angles.

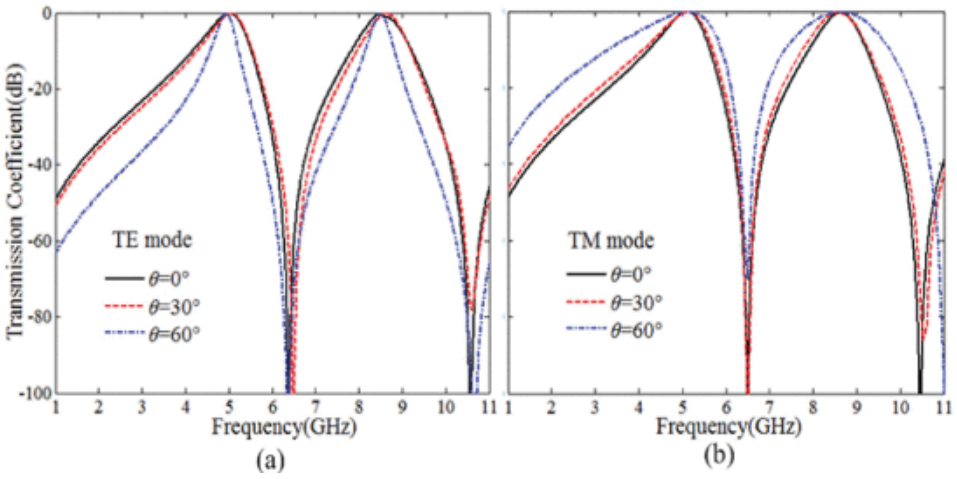

Fig. 1.29. Simulated results of reported FSS structure in [52], (a) TE (b) TM polarization.

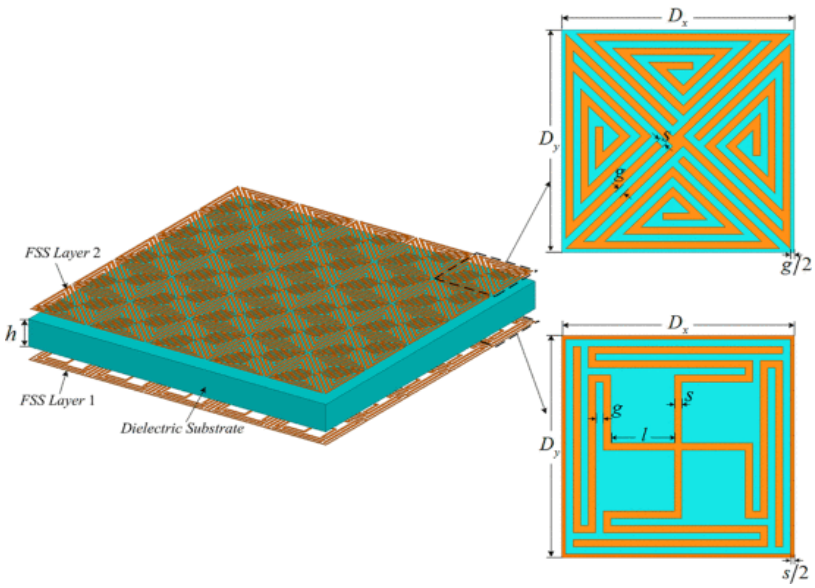

Fig. 1.30. Geometric configurations of the proposed FSS structure [53].

The described convoluted FSS in [53] is a low-profile structure comprising two periodic metallic arrays separated by a thin dielectric substrate (Fig. 1.30). The top metallic array features four branched spiral triangles connected at the center, while the bottom array consists of a gridded tortuous cross-dipole. This FSS design offers three passbands at 3.28, 4.2, and 5.4 GHz (Fig. 1.31). The proposed FSS demonstrates stable performance under oblique incidence for both TE and TM polarizations.

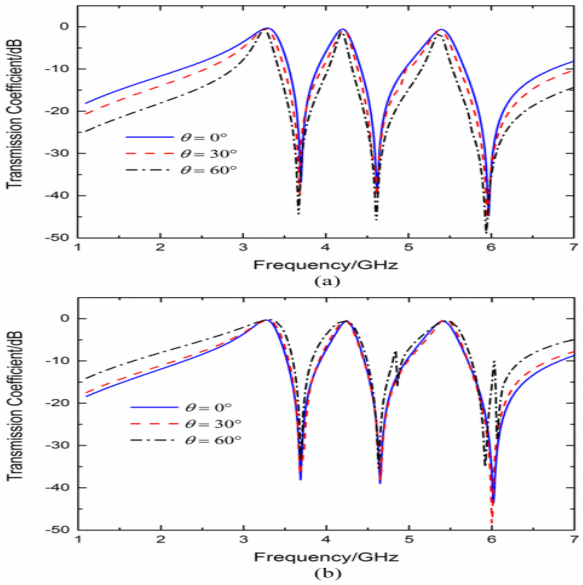

Fig. 1.31. Simulated results of the proposed FSS structure in [53], (a) TE (b) TM polarizations.

1.8.3. Fractal structures

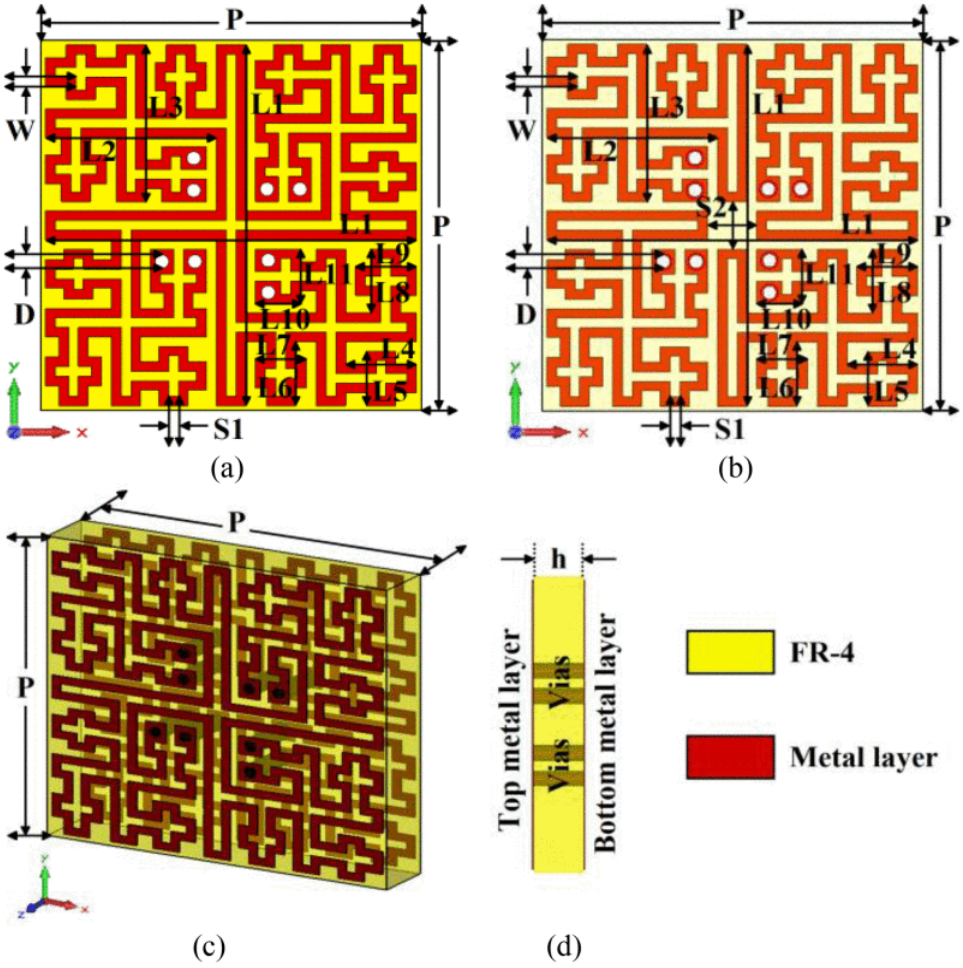

Fig. 1.32. Proposed structure [54], (a) top layer (b) bottom layer (c) 3-D view (d) side view.

Fractals emerge from geometric patterns through an iterative procedure repeated infinitely. Conversely, pre-fractal shapes result from truncating the iterative method after a finite number of iterations. The renowned characteristic of fractal Frequency FSSs lies in their self-similarity, leading to a multi-band response and compact design.

In reference [54], reported FSS incorporating four-legged loaded loop elements derived from a third-order iteration inspired by fractal geometries (Fig. 1.32). This FSS design aims to leverage the space-filling property inherent in fractals and an additional degree of freedom afforded by the use of metal vias in planar structures. The goal is to

achieve a miniaturized unit cell by enhancing the overall electrical length. The proposed FSS exhibits a band-stop (Fig. 1.33) response with resonance at 1.056 GHz and showcases identical transmission curves for both transverse-electric and transverse-magnetic modes of polarization in the incident wave.

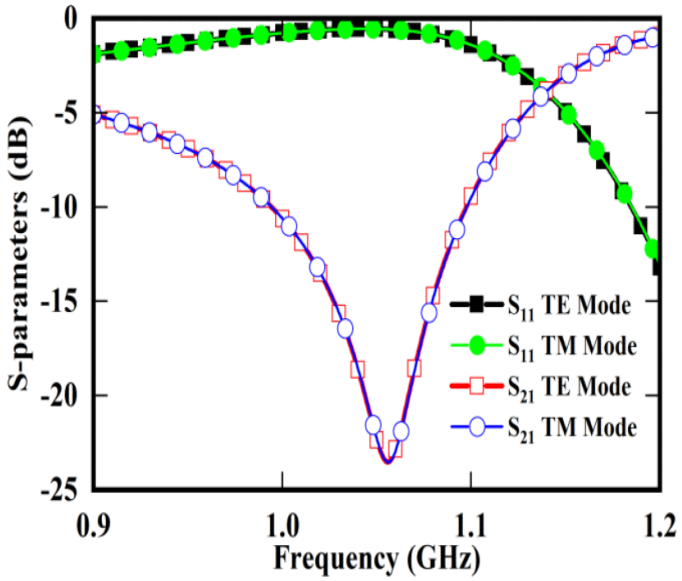

Fig. 1.33. Simulated results of proposed FSS in [54].

1.8.4. Switchable and Tunable Structures

Typically, conventional FSSs, comprising conducting patches and/or apertures on a dielectric substrate, exhibit a fixed performance due to their unalterable physical characteristics post-manufacturing. While their design and fabrication are relatively straightforward, certain applications necessitate adjustments to their frequency response. Addressing this challenge, Active Frequency Selective Structures (AFSS) emerge as a solution, enabling dynamic fine-tuning of EM performance through external excitations. In contrast to the static frequency characteristics of passive FSS, AFSS possesses reconfigurable EM properties, including resonant frequency and polarization, during operation. This reconfiguration feature is facilitated by the incorporation of active elements into the FSS structure. Common active elements in microwave AFSS include

On/Off switches, PIN diodes, varactor diodes, Schottky diodes, among others. The response of the AFSS undergoes changes when the state of such active devices (e.g., PIN diode) switches from ON to OFF or vice versa, contingent on the external DC bias source. Broadly, two categories of electrically controlled AFSSs are identified: switchable AFSSs and tunable AFSSs. The former toggles its response within the desired frequency band, alternating between transmission and reflection characteristics, while the latter can shift the resonant frequency within a specific frequency band.

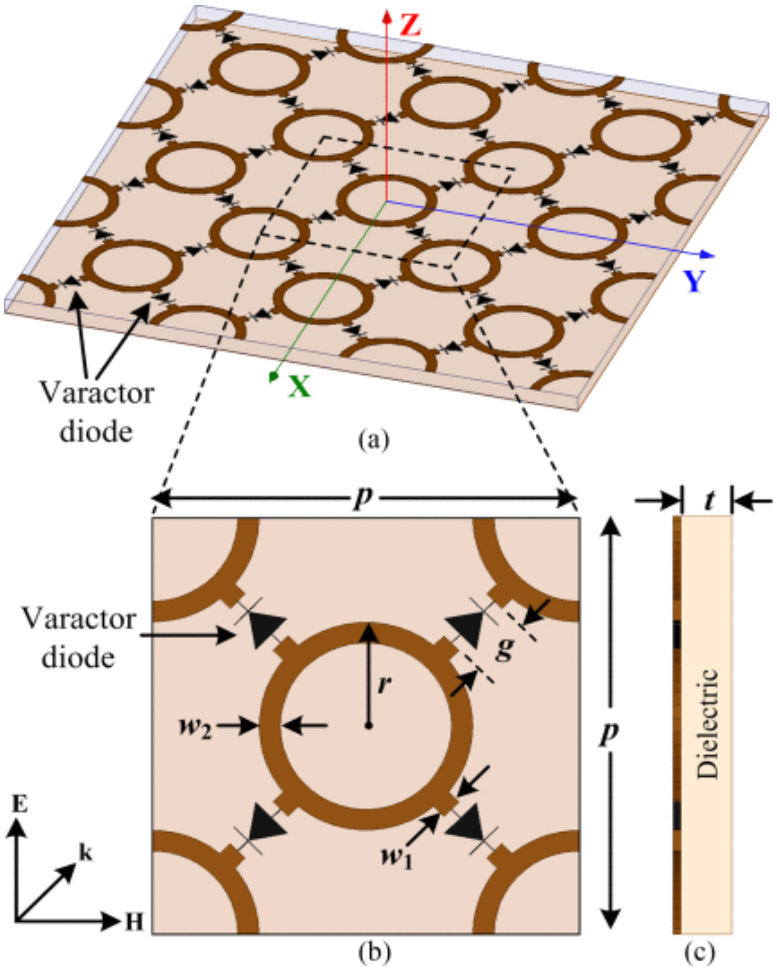

Fig. 1.34. Geometry of the proposed wideband tunable FSS [55]. (a) Perspective view. (b) Top and (c) side views of the unit cell structure.

The FSS [55] is composed of recurring arrangements of circular loops interconnected by varactor diodes (Fig. 1.34), demonstrating adjustable functionality. By applying a reverse bias voltage, the bandstop response can be manipulated within the

range of 0.54 to 2.50 GHz, showcasing a remarkable tunable span of 363%. This structure displays an expansive stopband of 1.28 GHz (with a fractional bandwidth of 152%), surpassing the capabilities of other wideband FSS designs (Fig. 1.35). Additionally, the design is characterized by its polarization-insensitivity and angular stability, accommodating both TE and TM polarizations.

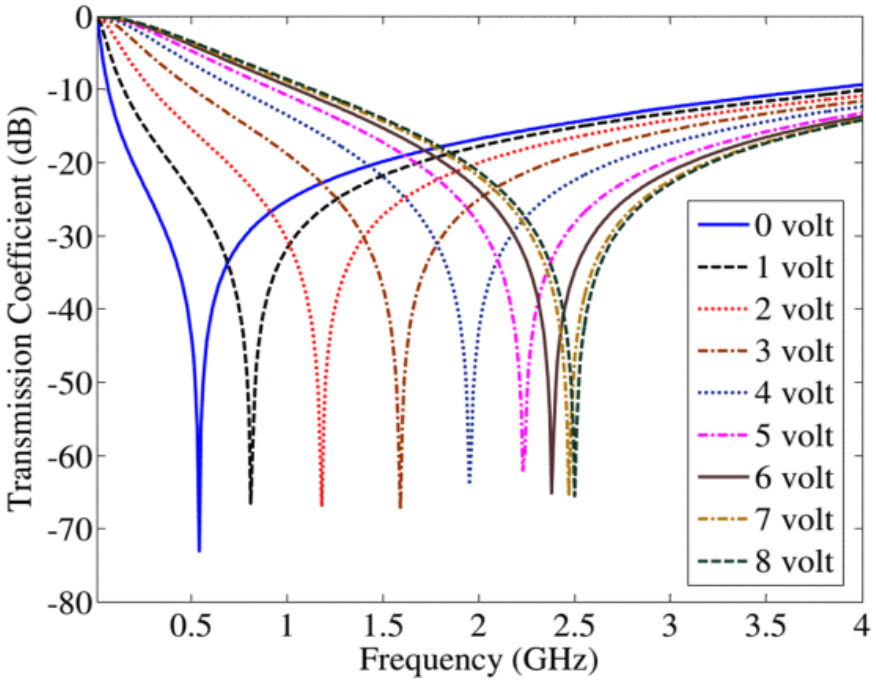

Fig. 1.35. Simulated results of the proposed structure [55] under different reverse bias voltages.

The absorber [56] is a multi-layer structure (Fig. 1.36), including the upper-layer Frequency Selective Surface, a lower-layer metal sheet, and an intervening air spacer. A single-chip microcomputer governs the biasing circuit, equipped with constant current outputs. Each output port links to a p-i-n diode, strategically employed to modulate absorption bands through precise control of induced current distribution. The system able to achieve rapid switching functionality within specific frequency intervals (3.62-5.35 GHz and 7.92-9.27 GHz), ensuring absorption depths beyond -10 dB (Fig. 1.37).

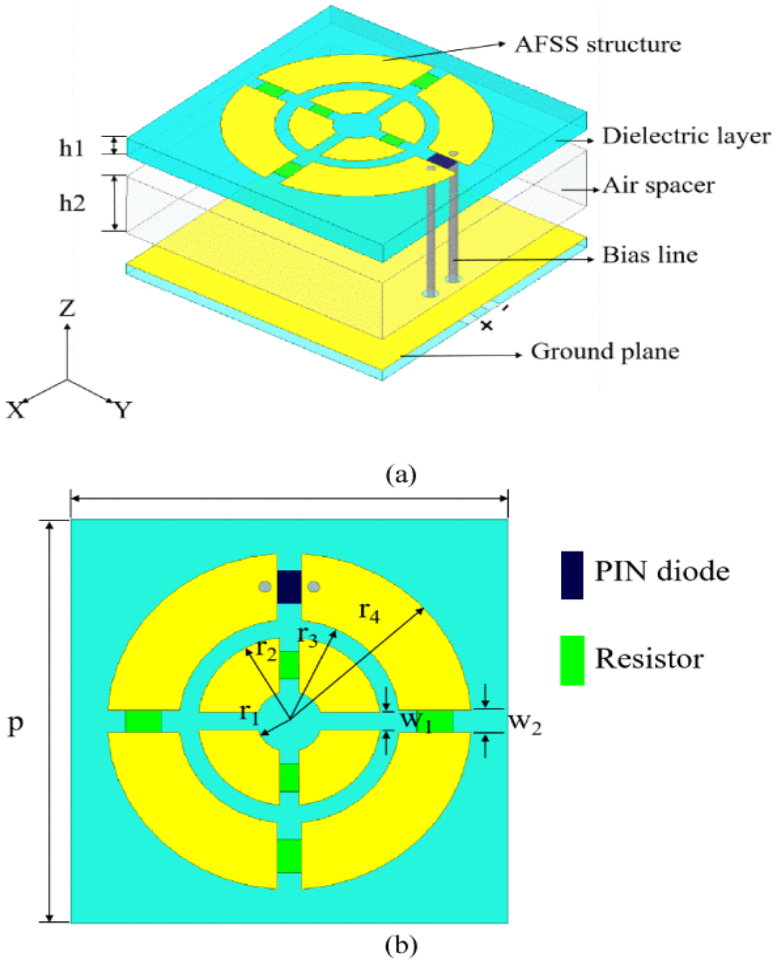

Fig. 1.36. Geometric structure of the AFSS absorber [56]. (a) Perspective view. (b) Top view.

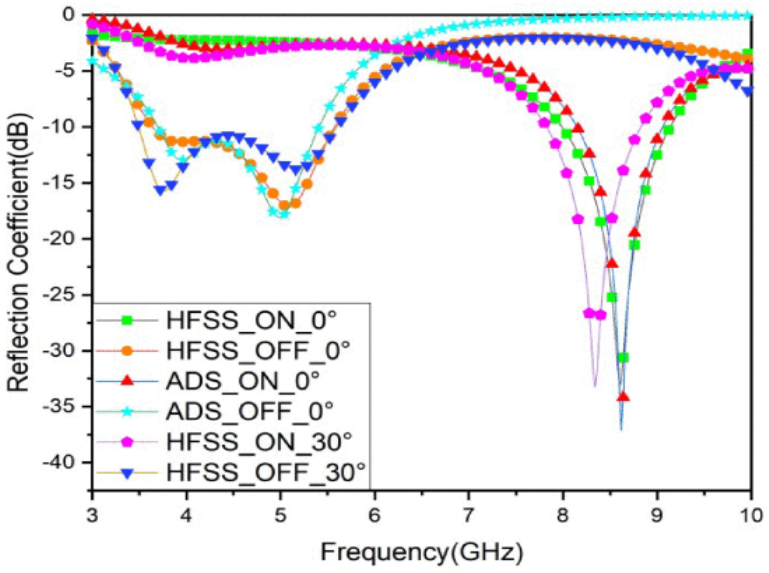

Fig. 1.37. Simulated results of the structure [56].

The publication [57] introduces a versatile polarization-insensitive multifunctional frequency-selective rasorber (MF-FSR). This innovative design is constructed with periodic metallic patterns on dual dielectric substrates, separated by an air spacer (Fig. 1.38). The distinctive feature of the MF-FSR lies in its ability to seamlessly switch between "rasorber mode (FSA-T)" and "absorber with notch band (FSA-N)" mode, providing real-time multifunctionality with continuous tunability in either the "transmission" or "notch" band.through the manipulation of the reverse bias voltage applied to the embedded varactor, the transmission band in FSA-T mode can be precisely tuned from 3.76 to 4.26 GHz, exhibiting an impressively low insertion loss ranging from 0.62 to 0.95 dB. In the complementary FSA-N mode, the notch band is also tunable within the range of 4.17 to 4.71 GHz. The same varactor set efficiently controls the tuning of either the transmission or notch band, depending on the MF-FSR's fundamental operational state, which is further independently adjustable through the incorporation of a p-i-n diode.

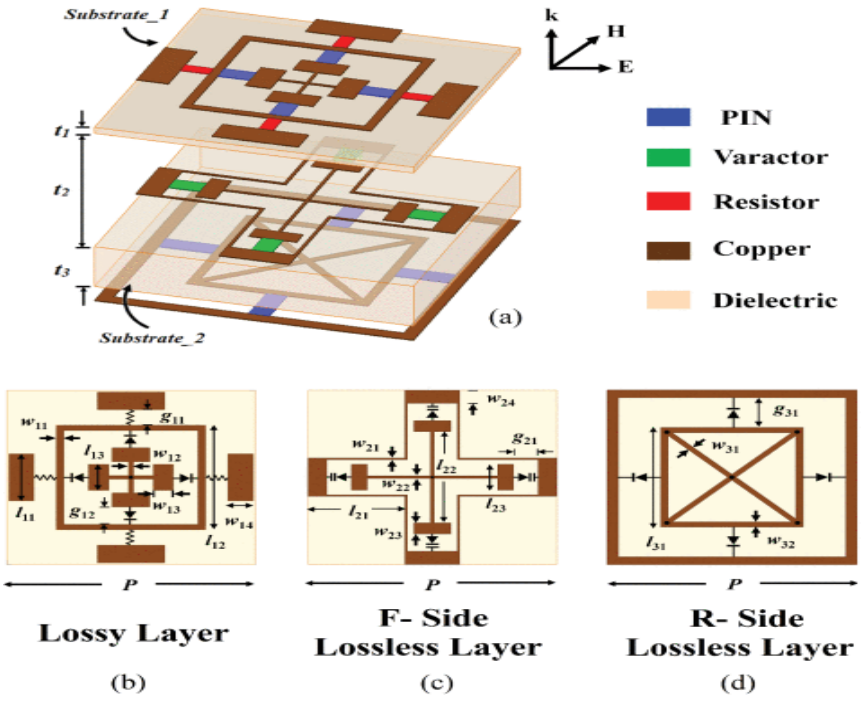

Fig. 1.38. Proposed multifunctional rasorber. [57] (a) Perspective view of the unit cell. (b) Lossy layer. (c) Front side (F-Side) and (d) Rear side (R-Side) of the lossless layer.

1.8.5. 3-D FSS Structures

To enhance the design of FSS, a departure from the conventional multilayer structure involves the incorporation of additional structures and cavities between planar layers, resulting in a novel 3D FSS configuration. Instead of the typical multilayer approach, the introduction of inter-structure elements offers a myriad of possibilities, such as periodic arrays of microstrip line boards, metal plate fragments, vias (holes), or resonating metal lines.

These innovative 3D configurations open up a realm of design possibilities, providing a surplus of methods for advanced performance characteristics. This adaptability is particularly advantageous for achieving in-band response stability, sharper cut-off, superior flexibility, and wider out-of-band rejection. The theory of cascading the cavity filters suggests that by strategically combining Substrate Integrated Waveguide (SIW) cavities within an FSS, the resulting selective performance can be truly remarkable, surpassing that of a single cavity FSS. This approach allows for a more nuanced and tailored approach to optimize the performance of FSS for specific applications.

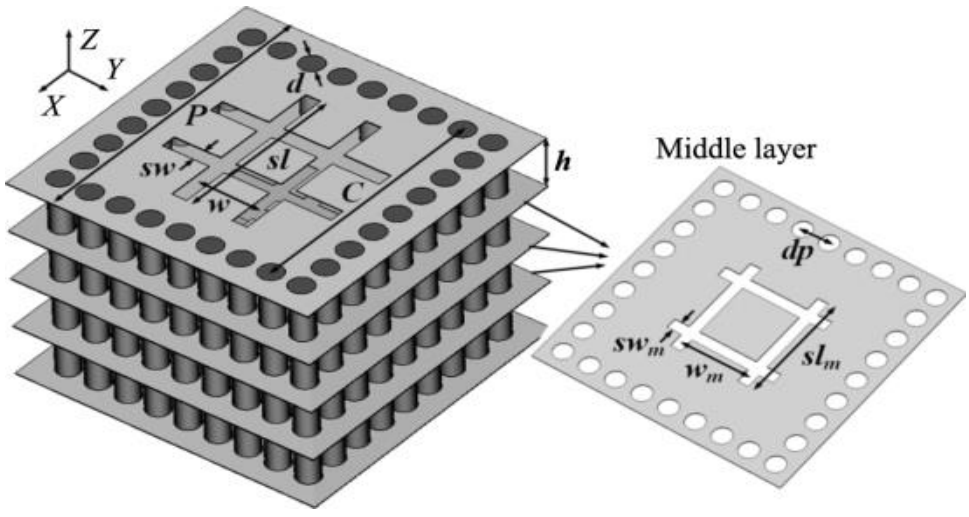

Fig. 1.39. Proposed SIW based FSS in [58].

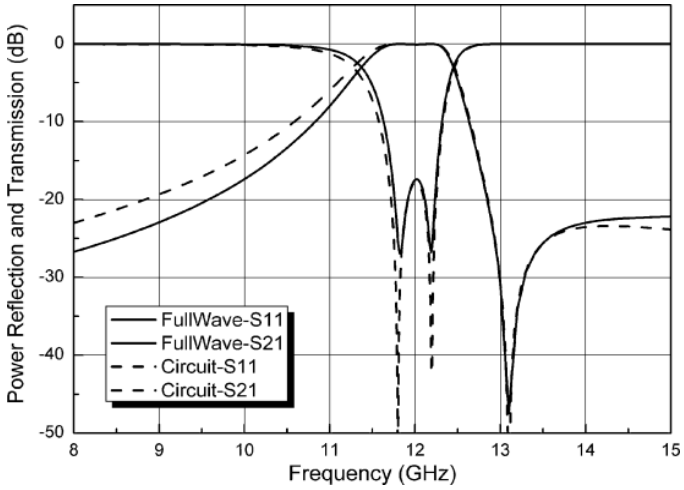

Fig. 1.40. Response of the proposed FSS structure in [58].

FSS utilizing a cascading structure of Substrate Integrated Waveguide (SIW) cavities (Fig. 1.39), documented in reference [58]. Through meticulous design and optimization, the selectivity performance of the FSS can be significantly enhanced. Notably, as the number of cascading SIW cavities increases, the FSS exhibits a more rapid roll-off on the sidebands, showcasing the potential for improved frequency selectivity with this approach (Fig. 1.40).

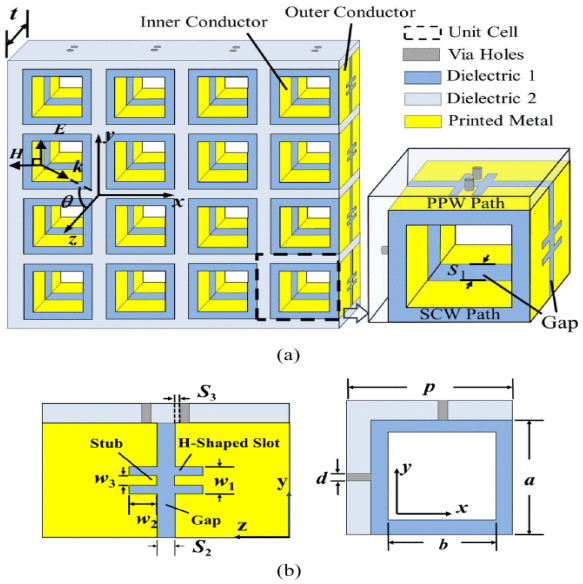

Fig. 1.41. (a) Perspective view of the proposed 3-D FSS and its unit cell [59]. (b) Geometry of the unit cell.

The 3D FSS proposed in [59] based on straightforward square coaxial waveguides. Within a single unit cell, the incorporation of via holes, H-shaped slots, and centered gaps is implemented to introduce additional resonances and couplings, thereby generating multiple transmission zeros and poles (Fig. 1.41). Consequently, this design yields two distinct passbands, each encompassing two transmission poles. Simultaneously, the presence of multiple transmission zeros facilitates a sharp roll-off in the rejection of the two passbands (Fig. 1.42), enhancing the overall performance of the FSS.

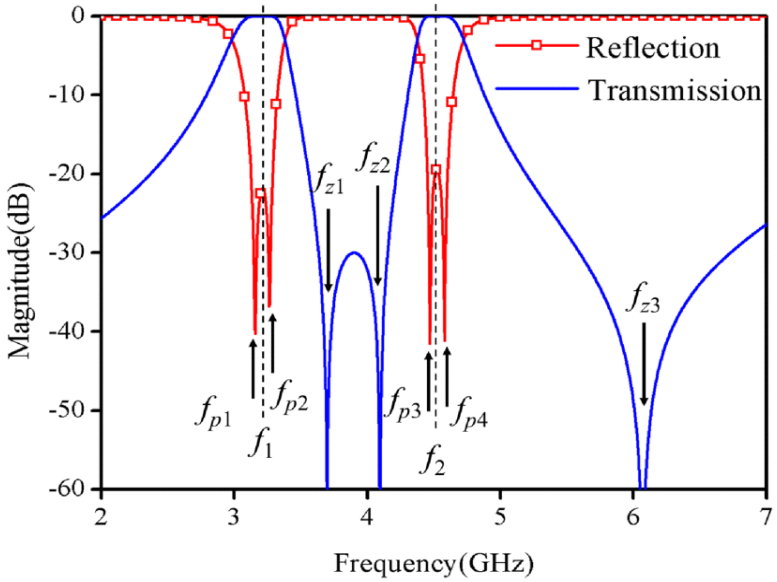

Fig. 1.42. Simulated results of the structure proposed in [59].

1.8.6. Conformal and wearable FSS

In the investigation presented in [60], a bandstop frequency selective surface with flexibility and frequency reconfigurability is examined (Fig. 1.43). The FSS structure is subsequently fabricated through additive printing using a fully automatic roll-to-roll screen printing machine (JOYSUN JYS-4070) on the surface of polyethylene terephthalate (PET). The conductive ink employed is a commercial silver nanoparticle. By biasing the embedded varactors within the range of 0 to 20 V, the measured resonant

frequency can be tuned from 3.5 to 5.7 GHz (Fig. 1.44). The resulting flexible FSS proves to be applicable in conformal scenarios, showcasing its adaptability for various practical applications.

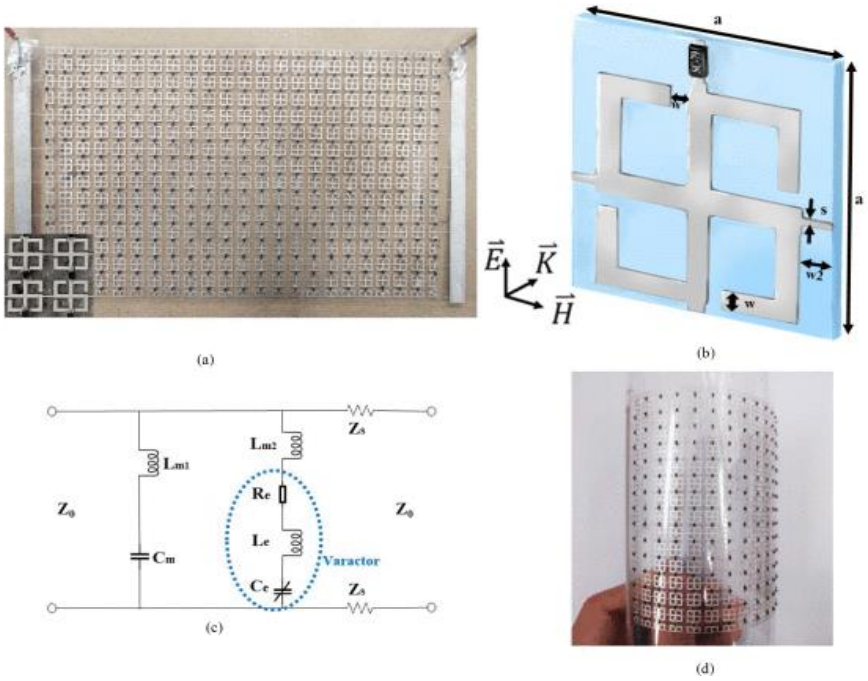

Fig. 1.43. Proposed conformal FSS in [60]. (a) FSS array (b) unit-cell (c) equivalent circuit (d) flexibility demonstration.

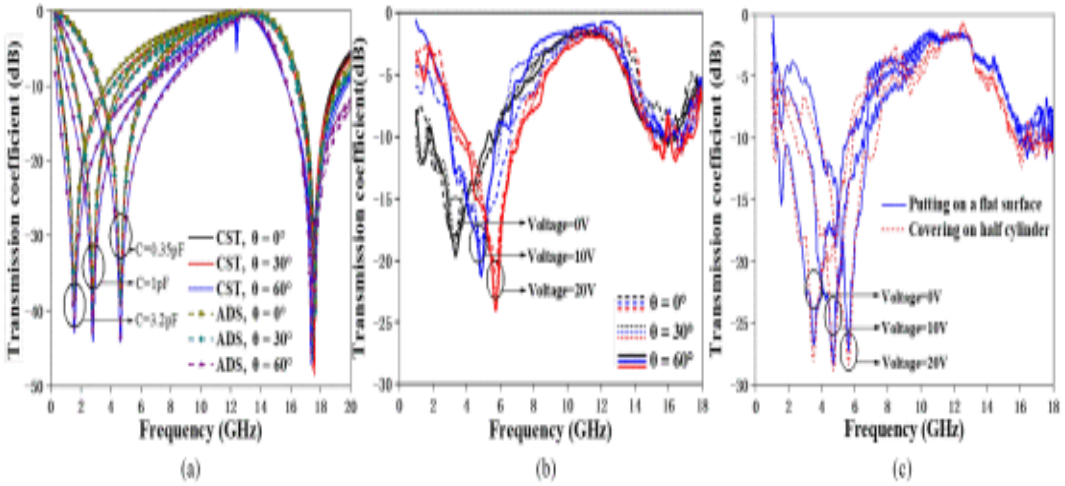

Fig. 1.44. Simulated results of the proposed conformal FSS in [60].

The comprehensive literature review for bandstop and bandpass FSS is given Table 1.1 and Table 1.2 respectively.

Table 1.1. Literature Review for Bandstop FSS

Ref No.	Title	Structure	Substrate, Unit-cell Area mm*mm	Frequency, (BW) In GHz	Maximum Angle of Incidence
[39]	A Frequency-Selective Wall for Interference Reduction in Wireless Indoor Environments	Square loops	Card Board 21*21	5.6-6	60
[61]	Analysis of Stop-Band Frequency Selective Surfaces with Dürer's Pentagon Pre-Fractals Patch Elements	Dürer's Pentagon Pre-Fractals Patches	FR-4 16.5*16.5	6.5	-
[62]	Optimal Design of Frequency Selective Surfaces with Fractal Motifs	Vicsek fractal	RT-duroid 6202 12.3*12.3	10.844 (0.894)	-
[49]	A Novel Dual-Band Angular Independent FSS With Closely Spaced Frequency Response	Two arm swasthik With meanderd arms	FR-4 10.4*10.4	2.54 3.54	60
[63]	A Miniaturized Flexible Frequency Selective Surface for X-Band Applications	Side bended square loop	FR-4 6.8*6.8	10 (8-12)	60
[64]	A Low-Profile Paper Substrate-Based Dual-Band FSS for GSM Shielding	Modified double square loop elements	Paper substrate 46*46	930M 1720M	60
[40]	Dual-band Single-Layer Quarter Ring Frequency Selective Surface for Wi-Fi Applications	Circular loops with inner circular arcs	FR-4 39.5*39.5	2.4 5.2	45
[65]	Stop band FSS with Ultra Large Angle of	Swasthik and ends extended	FR-4	7	80

	Incidence	with I Shaped strips	4.95*4.95	10.68 19.92	
[41]	WiMAX, WLAN, and X-Band Filtering Mechanism: Simple-Structured Triple-Band Frequency Selective Surface	Window type lines enclosed by square loops	FR-4 6.8*6.8	3.2-3.7 4.1-6 8-12.1	50
[66]	A Novel Dual-Band Ultrathin FSS With Closely Settled Frequency Response	Square patch with extended arms	Arlon Di 880 8.8*8.8	8.47 10.45	60
[67]	Easily Optimizable Dual-Band Frequency-Selective Surface Design	Concentric circular loops. Inner circle with splits	FR-4 29.3*29.3	2.4 5.8	60
[68]	A Design Method for Synthesizing Wideband Band-Stop FSS via Its Equivalent Circuit Model	(2)Square loops	F4B-2 6.8*6.8	13.5 88.9%	-
[69]	Miniaturised Bandstop Frequency Selective Surface Based on Quasi-Lumped Inductor and Capacitor	Meander line inductor, two layer capacitive square patch	Rogers 4003C 4.4*4.4	2.42 (0.32)	60
[42]	Novel Angular-Independent Higher Order Band-Stop Frequency Selective Surface for Xband Applications	Tilted cross dipole with extended folded arms	Arlon Di 880 7.7*7.7	9.9 (1.96)	60
[50]	An Angularly Stable Dual Band FSS with Closely Spaced Resonances Using Miniaturized Unit Cell	Two convoluted meandered patterns in each quadrant of unit cell	FR-4 8.4*8.4	2.35 3.05	60
[37]	Quad Band Polarization Insensitive Millimeter wave FSS for Remote	Circular loop with inner rectangular strips	Quartz 670u*670u	50-60(s) 87-91(s)	-

	Sensing			148-151(s) 175-195(p)	
[70]	A Triple Band Frequency Selective Surface Design for GSM Systems by Utilizing a Novel Synthetic Resonator	Rectangular shaped resonator and synthetic resonator	FR-4 50*50	942M 1842M 2142M	45
[71]	Design of Planar Dual-Bandstop FSS Using Square-Loop-Enclosing Superformula Curves	Square loops with Super formula curves	FR-4 10*10	3.46 5.14	60
[72]	Window RF shielding Film Using Printed FSS	Convoluted square loop with six meandered peaks	Polyethylene terephtalate 12*12	1.5-2.5	60
[55]	Brand band Polarization-Insensitive Tunable Frequency selective Surface for Wide band Shielding	Circular loops joined by PIN diods	FR-4 12*12	Tunable 0.55-2.52	60
[73]	A Wide band Frequency tunable FSS for Electromagnetic Shielding Applications	Mechanically Seperated Square loop Strips	FR-4 15*15	Tunable 3.5-8.2	-
[43]	Single-Layer Frequency Selective Surface With Angular Stability Property	Combination of Double Arc axisymmetric cross loop and Single arc centrosymmetric cross loop	2.2 0.001 8*8	5.94	85
[74]	Transmissive/Reflective FSS for Satellite Applications	Y Loops and Rectangular Curved Arms	Rogers 4003C 5*5	9.4(T) 14.5(R) 35(R)	80

Table 1.2. Literature Review for Bandpass FSS

Ref. No.	Title	Structure	Substrate, Unit-cell Area mm*mm	Frequency, (BW) In GHz	Maximum Angle of Incidence
[44]	A Frequency Selective Surface With Miniaturized Elements	Capacitive patches and Inductive grids	RO4003 8*8	14	45
[45]	A Second-Order Dual X-/Ka-Band Frequency Selective Surface	Jerusalem crosses embedded in sub wavelength capacitive patches	RO4003C 5*5	10 24	45
[46]	A Low-Profile Third-Order Bandpass Frequency Selective Surface	metallic patches and spiral square	RF-35 12.6*12.6	4 (20%)	50
[75]	A Miniaturized Dual-Band Frequency Selective Surface (FSS) With Closed Loop and Its Complementary Pattern	meandering loop	F4B-2 10.8*10.8	2.4 5.2	30
[76]	A Generalized Method for Synthesizing Low-Profile, Band-Pass Frequency Selective Surfaces With Non-Resonant Constituting Elements	Successive arrays of subwavelength capacitive patch	TPG-30 3.5*3.5	10.82 (21.7%)	-
[77]	Compound frequency selective surface with quasi-elliptic bandpass response	Cross slots	F4B-2 12*12	12.4 (2.8)	-
[78]	A Triband Second-Order Frequency Selective Surface	Circular strips and holes	FaB-2 20*20	9.45(0.47) 11.35(0.5) 13.4(0.64)	60
[79]	Synthesis of Quasi-Elliptic Bandpass Frequency-Selective	Square loop	Rogers 4230	5 (10%)	60

	Surface Using Cascaded Loop Arrays		18*18		
[51]	A Novel Miniaturized Frequency Selective Surface With Stable Resonance	Square spiral type	F4B-2 4.4*4.4	4	60
[80]	Multiband Metallic FSS with wide Range of Band Ratio	T Shaped Stubs	FR-4 12*12	8.7 9.6 11.1	45
[81]	A Miniaturized Dual-Band FSS With Second-Order Response and Large Band Separation	Square loops	F4B-2 3*3	8.9-11 30.1-33.6	60
[82]	A Tri-Band, Highly Selective, Bandpass FSS Using Cascaded Multilayer Loop Arrays	Square loops	F4B-2 5*5	7.1-8.1 11.8-13.4 18.3-19.7	60
[47]	A Quad-Band Frequency Selective Surface With Highly Selective Characteristics	Square loops	F4B-2 5*5	7.7 12.8 18.8 26.5	30
[83]	On the Improvement of Angular Stability of the 2nd-Order Miniaturized FSS Structure	Patches and Loops	F4B-2 5.8*5.8	10	60
[52]	A Miniaturized Dual-Band FSS With Controllable Frequency Resonances	Cross aperture element combined with meandered aperture element	F4B-2 6.6*6.6	5.13(1.27) 8.85(1.33)	60
[84]	A Low-Profile Miniaturized Second-Order Bandpass Frequency Selective Surface	Swasthik Capacitor layer, cross dipole inductive layer	FR-4 6*6	3.8 (10%)	60
[17]	Design and Analysis of Ultrathin Polarization Rotating Frequency Selective Surface Using V-Shaped Slots	V Shaped Slots	Rogers RT Duroid 5880 8.2*8.2	9.76-10.57	30

[85]	A Hybrid Miniaturized-Element Frequency Selective Surface With a Third-Order Bandpass Response	Inductive Grids and I Shaped Slots	Rogers RT Duroid 6010 7*7	8.1-8.9	45
[48]	A Bandpass FSS with a low Cross-Polarization Based on Cavities with a Hybrid Boundary	I Shaped Slots	Rogers 4003C 20*20	4.32-4.84	45
[86]	A Low Profile Broadband Bandpass FSS with Two Rapid Band Edges for 5G near field Applications	Metallic rings, swasthik shaped arms	Rogers RT Duroid 6.2*6.2	24.72-30.24 (20.5%)	40
[87]	An FSS Structure Based on Parallel LC Resonators for multiband applications	Patches and lines	Rogers 4003 6.5*6.5	2.45(0.93) 3.5(0.71) 5(1.11)	60
[88]	FSS Structure Miniaturization Using Interconnected Array Elements on Orthogonal Layers	Inter Connected Circular Loops	FR-4 10*10	2.4	60
[89]	Design of Dual Band Dual Polarization Transparent FSS	Line slot circular patch Enclosed by Rectangular Strips	F4B 9.8*9.8	7.63-8.97 13.26-13.87	-
[53]	A Miniaturized Triband FSS Based on Convoluted Design	Convoluted Design	F4B-2 6.2*6.2	3.28 4.25 5.42	60
[90]	An Ultrathin Bandpass FSS with Miniaturized Element	Meandered Square Loops	F4B-2	2	60
[10]	Design of FSS Structure with High Angular Stability for Radome Application	Gridded Square Loop, Cross Loop Aperture	F4B	15	60
[91]	A Low Profile Angel Insensitive Bandpass FSS Based ON vias	Swasthik	F4B	5	60

An FSS designed with a unit cell consisting of a circular loop with inner circular arcs is reported in [40] to stop both the 2.4 GHz and 5.2 GHz Wi-Fi frequency bands. The two-layer conducting FSS proposed in [41] features a square loop in the top layer and a square loop combined with two folded arms in the bottom conducting layer, operating across three distinct frequency bands: 3.2–3.5 GHz, 4.1–6 GHz, and 8–12.1 GHz, covering WiMAX, WLAN, and X-band within the specified frequency ranges. A novel angular-independent higher-order band-stop FSS for X-band applications is reported in [42]; the unit cell consists of cross dipoles with inward-curved arms. A modified double square loop structure is reported in [64] for GSM shielding. To stop ISM signal frequencies of 2.4 GHz and 5.8 GHz, a dual-band stop FSS is reported in [67], featuring concentric circular loops with inner circular arms.

A combined structure of two modified cross loops is reported in [43] for higher angular stability for a single stop band at 8.7 GHz. A stop-band FSS with a large angle of incidence up to 80° is presented in [65]; the unit-cell structure is swasthick and ends extended with I-shaped strips. FSS structures with vias are reported in [94] and [96] for large angular stability.

A gridded square loop and cross-loop aperture structure is reported in [10] for random applications. A bandpass FSS [98] for radome applications has been designed using a three-conducting-layer structure. SIW-FSS are presented in [99] and [100], while shorting vias are used in [98] and [101], and a 3-D structure is proposed in [102] for fast roll-off. However, these structures increase the complexity of the design.

1.9. Motivation and Objective

Research on FSS is primarily driven by its diverse applications where it can be effectively employed.

One prominent use of band-stop FSS is in electromagnetic shielding. Various studies in the literature have documented the implementation of band-stop FSS for GSM, Wi-Fi, WiMAX, WLAN, and X-band signals.

In recent times, the proliferation of satellites in space for communication and other purposes has seen exponential growth, with thousands already positioned in different orbits. Throughout the day, every geographical region on the Earth's surface falls within the footprint of numerous satellites. Consequently, electronic and communication systems are continually exposed to electromagnetic waves at satellite downlink frequencies. These signals have the potential to introduce noise, act as image frequencies, and alter the response of the system. Therefore, a key objective of the present thesis is to develop a band-stop FSS specifically designed to block certain satellite down-link frequencies.

In the literature, reported structures block various microwave frequencies, but no literature has reported structures that block satellite downlink frequencies. To achieve higher angular stability, complex structures have been reported [94], [95], [96]. For ease of fabrication and practical implementation, simple structures are necessary. If one wants to design a single elemental structure instead of dual elemental structures (e.g., two circular loops or two square loops for two bands), achieving two specific resonant frequencies is more difficult because tuning one desired frequency by changing the structure's dimensions may lead to the detuning of the other desired frequency so lot of optimization should be done to get two specific resonate frequencies.

The practical utilization of band-pass FSS is evident in their deployment within radomes. It would be very difficult for an enemy's radar to detect the presence of missiles, aircraft, submarines, and vehicles when stealth technology is used in their design and development. Recently, stealth technology has gained the attention of many

researchers because of its importance in defense. Radomes are used to protect electronic and communication systems in airborne radar systems. Radomes that are designed using FSSs pass only the desired frequencies and scatter the rest of the frequencies. Due to this characteristic of FSS radome, the radar cross-section of the radar antenna system is drastically reduced at out-of-band frequencies of FSS. Therefore, an FSS-based bandpass filter has become a promising electronic component for stealth applications. A crucial aspect of the design objective in this thesis involves creating a fast roll-off band-pass FSS tailored for application in stealth technology in X-band.

For a band pass FSS, achieving a fast roll-off requires increasing the filter's order, i.e., the number of slot layers. This is a disadvantage for band pass FSS because it increases the size of the structure. 3-D [102] and SIW [99][100] structures have been reported in the literature for fast roll-off. However, simple structures are more cost-effective and easier to fabricate than complex ones like 3-D and SIW. Obtaining a sharp roll-off simultaneously at both band pass edges with a simple structure is quite challenging. Achieving a sharp roll-off at one edge of the pass band may adversely affect the transmission characteristics of the pass band and the roll-off at the other edge. Therefore, significant optimization is required to meet the desired transmission characteristics of the structure.

1.10. Outline of the Thesis

The present thesis is structured into five chapters, and the chapter organization is as follows.

In the present chapter, the basic theory FSS has been discussed. A literature review is conducted on the design of different FSS structures.

In Chapter 2, the design of "Highly Angularly Stable Dual-Band Stop FSS for Blocking Satellite Downlink Frequencies" is presented.

In Chapter 3, the design of "A Novel Fast Roll-off Bandpass Frequency FSS for Stealth Applications" is presented.

In Chapter 4, the design of "Fast Roll-off Dual-Bandpass FSS" is presented.

In Chapter 5, the thesis's work is summarized, the key conclusions are made from the significant findings, and the possibilities for future exploration is presented.

1.11. Conclusion

In the current chapter, we delve into a brief historical overview of FSS and explore the fundamental theories associated with FSS. The chapter covers the essential principles behind bandstop and bandpass FSS filtering concepts. We also examine diverse designs of bandstop and bandpass FSS as documented in the literature review. Additionally, this chapter outlines the motivation behind the ongoing research and presents the objectives pursued in this study.